

~~SECRET~~  
FEB 18 1953

NACA TN 2896

# NATIONAL ADVISORY COMMITTEE FOR AERONAUTICS

TECHNICAL NOTE 2896

SURVEY OF PORTIONS OF THE IRON-NICKEL-MOLYBDENUM  
AND COBALT-IRON-MOLYBDENUM TERNARY  
SYSTEMS AT 1200° C

By Dilip K. Das and Paul A. Beck

University of Notre Dame



Washington

February 1953

FOR REFERENCE

NOT TO BE TAKEN FROM THIS ROOM

NACA LIBRARY

LANGLEY AERONAUTICAL LABORATORY  
Langley Field, Va.

## TECHNICAL NOTE 2896

SURVEY OF PORTIONS OF THE IRON-NICKEL-MOLYBDENUM  
AND COBALT-IRON-MOLYBDENUM TERNARY  
SYSTEMS AT 1200° C

By Dilip K. Das and Paul A. Beck

## SUMMARY

The 1200° C isothermal sections of the iron-nickel-molybdenum and the cobalt-iron-molybdenum ternary systems were surveyed. The phases occurring in these systems were identified by means of X-ray diffraction and by etching methods, and the phase boundaries at 1200° C were determined microscopically, using the disappearing phase method with quenched specimens. Both systems contain long solid-solution fields of the  $\mu$  phase. Other intermediate phases occurring in the iron-nickel-molybdenum system are the P phase and the delta phase. Both phase diagrams have extensive face-centered cubic solid-solution fields and some body-centered cubic solid solutions.

## INTRODUCTION

The present report is the last of four prepared for the National Advisory Committee for Aeronautics to cover research work conducted at the University of Notre Dame with the sponsorship and financial assistance of the NACA on phase diagrams of ternary and quaternary systems of interest in connection with high-temperature alloys. Previous reports of this series dealt with the chromium-cobalt-nickel system (reference 1), the chromium-cobalt-nickel-iron system (reference 2) and the chromium-cobalt-nickel-molybdenum system (reference 3). The main purpose of this work was to provide a survey of the phase relationships in these systems. In order to be able to complete such a survey within practicable periods of time, it was decided at the outset to do all work at a single temperature, with only supplementary data provided, wherever particularly desirable, at other temperatures. The temperature 1200° C was chosen for the isothermal survey work, since it is within the range of technologically useful annealing temperatures and it is high enough to allow a reasonable approach to equilibrium conditions in most alloys within a period of 1 or 2 days, thus allowing coverage of a wide composition range by processing a large number of alloys.

The work covered in the present report included two ternary diagrams, namely, the iron-cobalt-molybdenum and the iron-nickel-molybdenum. In view of the object of providing background information for high-temperature-alloy development, emphasis was placed on the face-centered cubic solid solutions. In addition to these, the boundaries of all phases were also investigated which are directly adjacent to the face-centered cubic phase and are capable of coexisting with it.

Following the nomenclature used in the previous reports, the face-centered cubic phase was designated alpha, and the body-centered cubic phase was designated epsilon. The intermediate phases covered in this investigation are the following: The delta phase based on the molybdenum-nickel binary phase at approximately 36 to 39 percent nickel, the mu phase based on the binary intermediate phase in the iron-molybdenum system at about 55 percent molybdenum and also occurring in the molybdenum-cobalt system at about 39 to 46 percent cobalt, and the newly discovered ternary P phase in the iron-molybdenum-nickel system. The mu phase in the iron-molybdenum system and in the cobalt-molybdenum system was designated by previous investigators (reference 4, p. 1210) as epsilon. The new nomenclature was adopted in order to avoid confusion with the body-centered cubic phase based on chromium, which occurred in the systems covered in the previous reports of this series. The mu phase also occurs in the iron-tungsten, the cobalt-molybdenum, and the cobalt-tungsten systems (reference 5). It has been designated by some investigators as xi. This phase has been reported to have a hexagonal structure with  $c/a = 5.4$  or, alternatively, a rhombohedral structure. The crystal structure of the delta and of the P phase is unknown. The P phase was recently discovered in the chromium-molybdenum-nickel system (reference 3) and is now found again as a ternary phase in the iron-molybdenum-nickel system.

The cobalt-molybdenum and nickel-molybdenum phase diagrams, discussed in reference 3, were determined by Sykes and Graff (reference 6) and by Ellinger (see reference 4, p. 1230), respectively. The cobalt-iron phase diagram was determined by Ellis and Greiner (reference 7) and the nickel-iron diagram is given in the "Metals Handbook" (reference 4, p. 1211). The only pertinent binary phase diagram not referred to in a previous report of this series is the iron-molybdenum phase diagram which is given in the "Metals Handbook" (reference 4, p. 1210). The only ternary phase diagram available in the literature for the iron-molybdenum-nickel system is that published by Köster (reference 8), and for the iron-molybdenum-cobalt system, the one published by Köster and Tonn (reference 9). The latter diagram was confirmed in its essential features. However, as described later, the phase diagram given by Köster for the iron-molybdenum-nickel system proved to be in error in several respects. Köster assumed that the molybdenum-iron mu phase and the molybdenum-nickel delta phase formed a continuous series of solid solutions. However, since that time it has become clear that these two

phases are not isomorphous and that, consequently, they cannot form a continuous series of solid solutions with each other.

The authors wish to express their appreciation of the assistance of Miss R. Kunkle and Messrs. J. R. O'Hara, G. R. Pendle, and M. Duggan.

#### EXPERIMENTAL PROCEDURE

A total of 170 alloys was prepared for the cobalt-iron-molybdenum and iron-nickel-molybdenum ternary systems. Of these, eight were in the iron-molybdenum binary system; that is, they were common to both the ternaries. Of the remaining alloys, 105 were in the iron-nickel-molybdenum system and 57, in the cobalt-iron-molybdenum system.

For the preparation and homogenization of the alloys the same experimental arrangement was used as described by Manly and Beck (reference 1). The melting was done in a high-frequency induction furnace under vacuum. Prior to the actual melting, while heating up the charge, several helium flushes were given. The charge was always 100 grams. The ingots were allowed to solidify in the crucible in vacuum. They were of cylindrical shape and varied from  $7/8$  inch to  $1\frac{1}{8}$  inches in diameter, depending on the crucibles used.

The ingots were found to be fairly free of segregation. The bottom part, which was comparatively more homogeneous than the top part of the ingot, was used for the investigation. The bottom sections of all ingots were sawed into four pieces. One of these was homogenized at  $1200^{\circ}\text{C}$  in a purified atmosphere consisting of a mixture of 92 percent helium and 8 percent hydrogen. A second piece, directly adjacent to the first, was used for chemical analysis.

The metals used for the preparation of alloys were (1) molybdenum in the form of  $1/8$ -inch rod, (2) electrolytic nickel, (3) electrolytic iron, and (4) cobalt rondelles. The lot analyses of the metals are given in table I. Three types of crucibles of approximately the same inside dimensions were used: (1) Recrystallized alumina, (2) Alundum, and (3) stabilized zirconia. Best results were obtained with the first two, and these were used in most cases. Table II lists the crucibles used for making each alloy.

Two different periods, namely 48 hours and 96 hours, were used for homogenizing at  $1200^{\circ}\text{C}$ . Experience in previous work on this project

showed that periods of this magnitude were sufficient for satisfactory approach to equilibrium conditions. The 48-hour homogenizing period was used for alloys consisting predominantly of alpha and/or epsilon phases, which could be hot-forged. These alloys were hot-forged twice at 1200° C, with a 1200° C anneal in between, prior to the homogenizing anneal of 48 hours. The other phases, namely, mu, P, and delta (and sometimes also epsilon), were too brittle to be hot-forged and consequently had to be homogenized for a longer period, namely, 96 hours. All alloys were quenched in cold water from the annealing temperature of 1200° C.

A powder sample for X-ray diffraction was prepared from each homogenized specimen by filing or crushing, depending on how ductile or brittle the specimen happened to be. The general rule was to use filing for alloys consisting predominantly of the alpha or epsilon phase. The other alloys were prepared by crushing. The rest of the homogenized specimen was used for microscopic investigation. The powder prepared for X-ray investigation was evacuated and sealed in a fused-quartz tube and heated at 1200° C for approximately 1/2 hour to relieve the strain of cold-working which arises in the preparation of the powder. At the end of the heating period the capsules were quenched in cold water.

Powder specimens were mounted on cardboard with collodion. The X-ray diffraction pattern was obtained in an asymmetrical Phragmen-type focusing camera of 20-centimeter diameter, using unfiltered chromium radiation at 30 kilovolts and 8 milliamperes. The camera covered an approximate range of  $\theta$  values of 18° to 78°. The primary importance of the diffraction patterns was identification of the phases when they occurred alone, or at least in appreciable amounts together with other phases. The method is rather insensitive in detecting small amounts of a second phase. A method of concentrating a brittle phase from the alloy powder, as described by Rideout and Beck (reference 3), was of considerable help in identifying small amounts of a second phase in an alpha matrix, when microscopic identification was doubtful. The presence of a small amount of a second phase, in the range of 0.1 to 0.2 percent was usually easily detected microscopically, but its identification was often quite difficult. Certain phases were recognizable in the as-polished condition in either bright field or oblique illumination (see, e.g., fig. 1). Others were detected by using various etchants. The following two etching reagents were most frequently used:

(1) The following etchant was used successfully in the cobalt-iron-molybdenum ternary system:

Hydrochloric acid saturated with cupric chloride, milliliters . . .	20
Ethyl alcohol, milliliters . . . . .	10

A stock solution of hydrochloric acid saturated with cupric chloride was made up and kept indefinitely without deterioration. Small amounts of the reagent were made ready for etching purposes as needed by mixing with ethyl alcohol. The best results were obtained by applying the etchant on a freshly prepared surface by swabbing with cotton. This etchant was useful primarily for the alpha phase, where it revealed grain boundaries, annealing twins, and transformation striations and also clearly delineated second-phase particles. It also attacked the epsilon phase to a certain extent, revealing its grain boundaries. Prolonged etching revealed the characteristic structure of the mu phase. This one etchant, and the use of as-polished surfaces, was sufficient for all microscopic work in the cobalt-iron-molybdenum ternary system. However, because of the presence of other phases, such as P and delta, in the iron-nickel-molybdenum system it was necessary to use additional etchants.

(2) Electrolytic etching followed by staining was used with success in the iron-nickel-molybdenum ternary system to distinguish between the intermediate phases. The following electrolyte was used under the conditions specified:

Phosphoric acid, milliliters . . . . .	5
Distilled water, milliliters . . . . .	95
Cathode . . . . .	Stainless steel
Voltage, volts . . . . .	4 to 6
Electrode spacing, inches . . . . .	1 to 2
Temperature . . . . .	Room
Time, seconds . . . . .	5 to 10

The electrolytic etch was followed by immersion for 30 to 60 seconds in an alkaline permanganate solution of the following composition:

Sodium hydroxide, grams . . . . .	10
Potassium permanganate, grams . . . . .	5
Distilled water, milliliters . . . . .	100

The electrolytic etch attacked the mu, P, and delta phases vigorously and the epsilon and alpha phases rather mildly. However, upon prolonged etching grain boundaries, transformation striations, and annealing twins in the alpha phase were revealed, although under such conditions the intermediate-phase particles were too strongly attacked and often altogether removed. This etchant was normally used under less severe conditions, where the mu phase was stained to a light tan color, with the grain boundaries revealed. The P phase showed a variety of colors ranging from gray, green, blue, yellow, and brown to pink. These colors were always very bright, the hue varying with the orientation of the P grains (figs. 2 and 3). The delta phase stained somewhat like the mu phase, usually to a bluish-gray color, varying only very slightly with orientation (fig. 4). Since the mu and delta phases did not coexist in

the system, differentiation between  $\mu$  and P and between  $\delta$  and P was sufficient so that no difficulty was encountered.

The  $\mu$ , P, and  $\delta$  corners of the three-phase fields  $\alpha$ ,  $\mu$ , and P and  $\alpha$ , P, and  $\delta$  were quite easily determined by microscopic identification alone. Some difficulties, however, were encountered in locating the  $\alpha$  corner of the various three-phase fields. Small amounts of the intermediate phases in an  $\alpha$  matrix were indistinguishable from each other by either etching method, although in larger sizes such particles were easily recognized. After the directions of the tie lines were determined and the other two corners of the three-phase fields were ascertained, the  $\alpha$  corners could be located.

In the cobalt-iron-molybdenum system the epsilon phase was mildly attacked by etchant 1, revealing grain boundaries (fig. 5). However, in a small region of the epsilon field, near the epsilon corner of the three-phase field  $\alpha$ ,  $\mu$ , and epsilon, the epsilon phase showed a dark staining effect (figs. 6 and 7). With a short etching time it became gray to brown, but upon longer etching the epsilon phase turned completely black. This effect was very useful in determining the location of the three-phase field.

In both the cobalt-iron-molybdenum and iron-nickel-molybdenum systems the  $\alpha$  phase near the iron corner transformed partially or wholly into epsilon upon quenching from 1200° C to room temperature. The X-ray diffraction patterns of such quenched specimens showed only epsilon or both epsilon and  $\alpha$  lines. It was, however, possible to differentiate microscopically between epsilon already present at 1200° C and that formed upon quenching, since the latter showed a typical acicular structure. Details of the microscopic method used will be discussed further below.

#### EXPERIMENTAL RESULTS

The microscopic and X-ray data for the phases occurring in the various alloys prepared are shown in tables III and IV. The isothermal sections for 1200° C, as shown in figures 8 and 9 for the cobalt-iron-molybdenum system and in figures 10 and 11 for the iron-nickel-molybdenum system, were drawn on the basis of these results. Most of the boundary alloys were analyzed for chemical composition. The acid-insoluble residue in the alloys varied between 0.1 and 0.5 percent. The compositions were recalculated on the basis of a total of 100-percent-metal content and are given in the tables in this form. For the alloys not chemically analyzed the tables give the intended composition. It was found that the deviations of the chemical analyses from the intended compositions were very small.

## Phases

The characteristics of the various phases occurring in the alloys investigated are described in the following paragraphs.

Alpha phase.- In the ternary systems the face-centered cubic alpha phase is based on the binary substitutional solid solutions of iron and nickel, and of iron and cobalt, respectively, with a certain amount of molybdenum in solid solution. The alpha phase alloys are ductile and could be easily hot-forged before homogenizing. Etchant 1 was used to bring out the microstructure, which is typical of face-centered cubic metals, showing equiaxed grains abounding in annealing twins (fig. 12).

The iron-rich solid solutions, which have the face-centered cubic alpha structure at 1200° C, partly or wholly transform upon quenching to room temperature. Addition of nickel or cobalt in small amounts does not suppress this transformation. The microstructures of such specimens show characteristic acicular structures or transformation striations (figs. 13 and 14). The individual alpha grains, which existed at 1200° C, could be recognized from the directions of the transformation striations. The grains are comparatively much larger for the alloys which consist of a single phase at 1200° C (regardless of whether alpha or epsilon) than for those with two phases at the annealing temperature.

The X-ray diffraction lines of the epsilon phase are quite sharp when the epsilon phase exists at the temperature of homogenization and is retained by quenching. However, the epsilon lines are very broad and diffuse when the epsilon phase is formed partly or wholly by transformation from alpha during quenching. The acicular microstructure and the broadening of the diffraction lines allow positive distinction between epsilon formed by transformation upon quenching and epsilon present at 1200° C before quenching. By means of these criteria the alpha phase boundaries at 1200° C could be determined. Table V gives the data from a typical X-ray diffraction pattern of the alpha phase.

Epsilon phase.- In both ternary systems the epsilon phase is based on the body-centered cubic solid solutions of molybdenum in iron. Although alloys of this phase are quite ductile in comparison with the intermediate phases, they are not so ductile as the alpha phase. Epsilon alloys could be usually hot-forged.

The microstructure of the single-phase epsilon alloys revealed large equiaxed grains (fig. 5). No Widmanstätten pattern could be detected by using either etchant. This fact lends further support to the view that the Widmanstätten structures previously found in the epsilon phase in the chromium-cobalt-nickel (reference 1), chromium-cobalt-iron (reference 2), and chromium-nickel-molybdenum (reference 3) systems were due to the precipitation of the sigma phase. In the



iron-nickel-molybdenum and iron-cobalt-molybdenum systems the sigma phase does not coexist with the epsilon phase, as it does in the other systems mentioned. Table VI gives the data of a typical X-ray diffraction pattern for the epsilon phase.

Mu phase.- In this investigation it was found that the composition of the cobalt-molybdenum mu phase varied between about 39 and 46 percent cobalt at 1200° C. The composition of the iron-molybdenum mu phase was about 43 to 47 percent iron. Henglein and Kohsok (reference 5) stated that the cobalt-molybdenum mu phase is isomorphous with the corresponding intermediate phases in the iron-molybdenum, iron-tungsten, and cobalt-tungsten systems. In the course of the investigation of the iron-nickel-molybdenum system it was found that the iron-molybdenum mu phase took a certain amount of nickel in solid solution and extended toward the nickel-molybdenum binary. In the cobalt-iron-molybdenum system unlimited solid solubility was found between the iron-molybdenum and cobalt-molybdenum mu phases, the mu phase field running approximately parallel to the iron-cobalt side.

The crystal structure of the mu phase can be described as hexagonal or rhombohedral (reference 5). The data for a typical X-ray diffraction pattern of this phase appear in table VII.

To reveal the microstructure of the mu phase, etchant 2 was used, followed by a staining treatment. The mu phase has a very characteristic microstructure (fig. 15), which at a casual glance could give the impression of a two-phase alloy. The same characteristic microstructure was previously found for the mu phase in the chromium-cobalt-molybdenum and cobalt-nickel-molybdenum systems (reference 3). Certain grains are attacked preferentially by the etchant, depending on their orientation. The alkaline permanganate stain gives various shades of light to dark tan for different grains in the same specimen. Etchant 1 was used for the mu phase in the cobalt-iron-molybdenum system; the action was very slow, but eventually it brought out the same characteristic structure as described above. This etchant can be used to delineate the boundaries of mu-phase particles in a matrix of epsilon (fig. 16).

The mu phase did not stain to any vivid colors when it was in a matrix of the P phase or when it formed the matrix and the second phase was either alpha or epsilon. However, when the mu was the minor phase in a matrix of alpha (fig. 17), it stained to vivid bright colors, similar to those shown by the P-phase, and it was thus hard to distinguish from the latter. In such circumstances, X-ray identification had to be resorted to.

Delta phase.- The delta phase was previously reported to occur in the chromium-nickel-molybdenum and cobalt-nickel-molybdenum systems (reference 3). In the present investigation it was found in the

iron-nickel-molybdenum system. In all three cases it is based on the corresponding intermediate phase of the nickel-molybdenum binary system. It is a hard and brittle phase, although apparently not quite so brittle as the P or the  $\mu$  phase. Microscopic identification of the delta phase in the presence of P or of alpha is not difficult if the stain-etching procedure (2) is used (fig. 18).

The crystal structure of the delta phase is not known, and the diffraction pattern is quite different from that of the  $\mu$  phase. The very large number of lines in the pattern suggests a large unit cell. Typical diffraction-pattern data for this phase appear in table VIII.

P phase.— The P phase was first discovered (reference 3) as a ternary phase in the 1200° C isothermal section of the chromium-nickel-molybdenum system; it is not known to exist in any of the binary systems involved. In the course of this investigation a ternary phase of the same structure was found to occur also in the 1200° C section of the iron-nickel-molybdenum system in a narrow range of compositions between the  $\mu$  and delta phases. Etchant 2 was used for the identification of this phase. It stained to brilliant hues varying from gray-blue, blue, yellow, and green to pink. The greatest color effect is observed when the P phase occurs together with other phases (fig. 3). The great variation of shading and hue of the stain in adjacent grains of the same phase may be attributed to an orientation effect.

The X-ray diffraction pattern of this phase was recently published (reference 10). The crystal structure has not been determined. Table IX gives the data from a typical X-ray diffraction pattern of the P phase.

Z phase.— Kamen and Beck (reference 2) found a set of unidentified lines, occurring always in a group, in the patterns of certain alpha alloys of the quaternary cobalt-chromium-iron-nickel system. The lines appeared only when the powder was prepared for the X-ray diffraction work by filing. Upon preparing the powder by crushing, the lines never appeared. No microscopic evidence of this phase was ever observed. The following alloys in the iron-nickel-molybdenum ternary system showed the lines of the Z phase: 702, 701, 704, 705, 706, and 707. Lines observed in the above alloys consisted of alpha and Z lines only. The diffraction lines of the Z phase are shown in table X. As identified microscopically, there were appreciable amounts of the  $\mu$ , P, and delta phases present in these alloys, but in the X-ray diffraction patterns obtained from filed powders the lines of these intermediate phases were not found. Then X-ray diffraction powder samples were prepared by crushing the alloys; the intermediate-phase lines appeared in accordance with the microstructure, with a complete absence of the Z phase lines. In an attempt to identify the Z phase, diffraction patterns were prepared from the following materials: (a) A powder sample of the file used for filing the alloys in question; (b) a powder sample of a nickel-molybdenum beta

phase alloy, 28 percent molybdenum plus 72 percent nickel, annealed at 800° C for 1 week; and (c) a powder sample of the nickel-molybdenum gamma phase, 35 percent molybdenum plus 65 percent nickel, annealed at 800° C for 1 week. None of these diffraction patterns contained the Z phase lines; the origin of these lines remained obscure.

### Phase Diagrams

Cobalt-iron-molybdenum ternary system at 1200° C.— The 1200° C isothermal section of the cobalt-iron-molybdenum ternary system (fig. 8) is drawn in accordance with the data given in table III. The same phase diagram is shown in figure 9, together with the alloy compositions used. Since the purpose of this investigation was to determine the boundaries of the face-centered alpha solid solutions and of the phases nearest to these solid solutions, the highest percentage of molybdenum used was 62 percent. The highest-molybdenum-containing alloys were needed in order to find the high-molybdenum boundary of the mu phase. The iron-molybdenum binary diagram (reference 4, p. 1210) is known (reference 11) to have a sigma phase at about 63 percent molybdenum, in a narrow composition range. However, since this phase does not coexist with the alpha solid solutions at 1200° C, its boundaries in the ternary systems were not investigated.

Within the ternary composition range covered in the present work, the phases found at 1200° C were those that occur in the binary systems concerned, namely, the face-centered cubic alpha phase, based on the solid solutions of iron and cobalt, the body-centered cubic epsilon solid solutions of molybdenum and iron, and the mu phase.

The alpha phase is bounded by the cobalt-iron binary system; on the iron-molybdenum side it extends from the iron corner to 2.0 percent molybdenum and on the cobalt-molybdenum side, from the cobalt corner to 22.5 percent molybdenum. The ternary alpha solid solutions are bounded by two slightly concave lines meeting at the point 58.6 percent iron, 17.0 percent molybdenum, and 24.4 percent cobalt, which is the alpha corner of the alpha-mu-epsilon three-phase field.

The epsilon phase field extends along the iron-molybdenum binary system from 4 to 21 percent molybdenum, and it terminates at the epsilon corner of the alpha-mu-epsilon three-phase field at 60 percent iron, 19 percent molybdenum, and 21 percent cobalt.

The mu phase field extends from the iron-molybdenum side to the cobalt-molybdenum side, approximately parallel to the cobalt-iron boundary. The mu corner of the alpha-mu-epsilon three-phase field is at approximately 29.4 percent iron, 51.6 percent molybdenum, and 19.0 percent cobalt.

The alpha phase coexists with the epsilon phase in a curved narrow two-phase field and with the mu phase along a wide two-phase field. Epsilon and mu coexist with each other over a comparatively wide range of compositions. All the three phases coexist in a long and narrow three-phase field. The alpha and epsilon corners of the three-phase field as well as both boundaries of the alpha-epsilon two-phase field had to be determined entirely by microscopic methods; X-ray investigation in this region failed because of the transformation of the alpha phase into epsilon upon quenching to room temperature. However, microscopically the transformed alpha grains could be easily distinguished from the epsilon grains, which remained unchanged upon quenching from 1200° C to room temperature (figs. 5, 14, 19, and 20). Even in the presence of large amounts of the mu phase, when the alpha and epsilon grains were very small, the alpha grains were recognized by their roughened appearance upon etching with the reagent 1, while the epsilon grains were smooth.

Determination of the mu corner of the three-phase field was carried out by a combination of three different methods. A few alloys containing appreciable amounts of mu were studied microscopically, but this method gave only a rough approximation, because of the difficulty of microscopic distinction between the alpha and epsilon phases when they were present in small amounts. For more accurate determination, the  $d$  spacings calculated from the twenty-ninth line (table VII) of the saturated mu phase boundary alloys were plotted against the cobalt content. (See fig. 21, data in table XI.) A break in the curve of parameter against composition was found at 19 percent cobalt. Verification of this result was obtained by determining the  $d$  value for the same diffraction line with alloy 852, which was microscopically found to contain all three phases. This  $d$  value turned out to be very nearly the same as that obtained at 19 percent cobalt in the above curve, indicating that this point is at the mu corner of the three-phase field. Table XII shows the variation with alloy composition of the lattice parameter of the saturated ternary alpha phase. The results obtained from alloys 745 and 800 are not very reliable because of partial transformation. It is seen that along the boundary the unit cell expands as the cobalt content decreases.

In general, the present data are quite consistent with the published data for the binary systems, although there are some minor discrepancies. The mu phase field in the cobalt-molybdenum system was found to extend from about 39 to 46 percent cobalt, rather than from 38 to 44 percent, as given by Sykes and Graff (reference 6). Similarly, in the iron-molybdenum system the mu phase was reported to extend from about 54 to 55 percent molybdenum, while the limits established in the present work are 52.5 to 57 percent molybdenum. The solubility limit of molybdenum in epsilon at 1200° C was previously set at about 19 percent, and it is now determined to about 21 percent molybdenum. The 1300° C isothermal

section of the iron-cobalt-molybdenum system published by Köster and Tonn (reference 9) gives somewhat higher solubilities for molybdenum in both alpha and epsilon than those found in the present work for 1200° C. This difference may well be due to the increase in solubility with increasing temperature. Köster and Tonn's diagram places the  $\mu$  corner of the three-phase field at about 6 percent cobalt, in contrast with 19 percent cobalt found for this corner point in the present work.

Iron-nickel-molybdenum ternary system at 1200° C.— The 1200° C isothermal section of the iron-nickel-molybdenum ternary system, as drawn from the data in table IV, is presented in figure 10. The same phase boundaries together with the compositions of the alloys used in this investigation are plotted in figure 11. Here, too, as in the iron-cobalt-molybdenum system, only the boundaries of the alpha solid solutions and of the phases adjacent to alpha were investigated; the highest percentage of molybdenum used was 64.5 percent. The following single-phase, two-phase, and three-phase fields occur and were determined in the course of this investigation:

Single-phase fields: Alpha, epsilon,  $\mu$ , P, and delta

Two-phase fields: Alpha plus epsilon, alpha plus  $\mu$ , alpha plus P, alpha plus delta, epsilon plus  $\mu$ ,  $\mu$  plus P, and P plus delta

Three-phase fields: Alpha plus epsilon plus  $\mu$ , alpha plus  $\mu$  plus P, and alpha plus P plus delta

The alpha phase field, which is the most extensive, is based on the austenitic solid solutions of iron and nickel, which are uninterrupted at 1200° C. The maximum amount of molybdenum going into solution in this phase was found to be 35.5 weight percent at the nickel-molybdenum binary edge. The minimum of 2.0 percent molybdenum is at the iron-molybdenum side. In the 1200° C ternary section the boundary consists of: (1) An almost straight line, separating the alpha field from alpha-plus-epsilon field and terminating at 72.7 percent iron, 15.7 percent molybdenum, and 11.6 percent nickel (alpha corner of alpha-plus-epsilon-plus- $\mu$  three-phase field); (2) a concave line from this corner point to the alpha corner of the alpha-plus- $\mu$ -plus-P three-phase field at approximately 16 percent iron, 28.5 percent molybdenum, and 55.5 percent nickel; and (3) a concave line from the latter point to the binary nickel-molybdenum solubility limit at about 35.5 percent molybdenum. In this ternary system, as in the cobalt-iron-molybdenum system, the alpha phase alloys near the epsilon phase field transformed into epsilon phase upon quenching from 1200° C to room temperature. The 1200° C phase boundaries were again determined by the microscopic method described above in connection with the cobalt-iron-molybdenum system.

At 1200° C the epsilon phase extends from the binary iron-molybdenum ferritic solid solutions (from 4 to 21 percent molybdenum) to the epsilon corner of the alpha- $\mu$ -epsilon three-phase field, tentatively indicated

at 8 percent nickel, 71 percent iron, and 21 percent molybdenum. It is probable that this corner point is actually located at a somewhat higher molybdenum content.

The  $\mu$  phase, based on the intermediate phase in the iron-molybdenum system, penetrates deep into the ternary system up to a maximum nickel content of about 19.4 percent, while the iron content decreases to about 23 percent. The elongated  $\mu$  phase field is approximately parallel to the iron-nickel side of the diagram. As nickel is substituted for iron in forming the  $\mu$  phase, the lattice of the latter expands. (See table XIII.) Upon further addition of nickel in place of iron, the  $\mu$  phase terminates and P begins to form. This is a ternary phase previously reported (references 3 and 10) to occur in the chromium-nickel-molybdenum system also as a ternary phase. When the nickel-iron ratio is further increased, the P phase is replaced by delta, based on the intermediate phase in the binary molybdenum-nickel system, which can dissolve a maximum of only 8.5 percent iron. The  $\mu$ , P, and delta phases, together with the two two-phase fields between them, occupy a narrow strip running roughly parallel to the nickel-iron edge of the ternary diagram, somewhat as the uninterrupted  $\mu$  phase field does in the cobalt-iron-molybdenum system.

All three intermediate phases are hard and brittle, delta apparently being the least brittle of the three. Their hardnesses appear to be of about the same order, since no relief effect was observed in the as-polished condition between either P and  $\mu$  or P and delta.

The location of the  $\mu$  corner of the alpha- $\mu$ -epsilon three-phase field was verified by plotting the  $d$  spacing of line 29 (table VII) for the saturated alloys at the low-molybdenum boundary of the  $\mu$  phase against the nickel content (fig. 22, table XIV). A break in the curve appears at 5 percent nickel, corresponding to the three-phase-field corner, as located microscopically. Table XIII shows that for the alpha alloys saturated with molybdenum there is a general tendency for lattice shrinkage with decreasing nickel content. The X-ray diffraction patterns of alloys 801, 802, and 838, and of all alloys with lower nickel content, had only epsilon lines, while the patterns of alloys 723 and 722 had a mixture of alpha and epsilon lines. It is clear that the lattice parameter of the alpha phase around the iron corner cannot be determined by room-temperature X-ray diffraction work. Consequently, the alpha corner of the alpha-epsilon- $\mu$  three-phase field could not be checked by X-ray diffraction. Because of the small number of available alpha boundary alloys, in determining the alpha corners of the other two three-phase fields only the microscopic method could be used. Table XV gives the location of the corners of the three-phase fields.

## DISCUSSION

From the point of view of useful application to high-temperature alloys, the face-centered cubic alpha (austenitic) solid-solution field is of the greatest importance. It is seen in figures 8 and 10 that the addition of iron decreases the solubility of molybdenum in both the molybdenum-cobalt alpha and molybdenum-nickel alpha phases. However, uninterrupted austenitic solid-solution fields exist at 1200° C in both ternary phase diagrams all the way to the iron corner. The solubility of molybdenum in the austenitic solid solutions is limited near the iron corner by equilibrium with the body-centered cubic epsilon phase (ferrite). Also, in both ternary diagrams near the alpha-plus-epsilon two-phase field the alpha solid solutions transform wholly or partially into the epsilon phase upon quenching from 1200° C to room temperature. Such alloys give room-temperature X-ray diffraction patterns consisting of the epsilon or the epsilon and alpha lines. The microscopic method described in a previous section is, however, capable of detecting the conditions existing at 1200° C before quenching. This is possible because of the occurrence of characteristic acicular transformation structures in alloys which consist of alpha at 1200° C but transform upon quenching. The approximate ranges of the alpha solid-solution fields, where this transformation occurs, are marked "A" in both phase diagrams (figs. 8 and 10).

The results obtained in the present investigation for the iron-molybdenum-cobalt system (fig. 8) agree reasonably well with those obtained by Köster and Tonn (reference 9); the general features of the two ternary phase diagrams are the same. Differences in the locations of the boundaries might be a result of the fact that the boundaries in the present investigation were determined for 1200° C, while Köster and Tonn's investigation gave the boundaries at 1300° C.

The iron-nickel-molybdenum ternary diagram obtained in the present investigation is considerably different from the diagram published by Köster (reference 8). Köster's diagram indicates a continuous series of solid solutions between the iron-molybdenum and the nickel-molybdenum intermediate phases next to the iron and nickel corners, respectively, of the diagram. It has been known, however, from more recent work (reference 3) that these two binary intermediate phases are not isomorphous; consequently, it was expected that they will not form a continuous series of solid solutions. In the present investigation it was found that the iron-molybdenum mu phase does not even coexist with the nickel-molybdenum delta phase. The two are separated by a ternary phase, isomorphous with the ternary P phase previously identified in the chromium-nickel-molybdenum system. The ternary P phase in both systems has a relatively small composition range. It is quite possible, however, that these two isomorphous ternary phases form a narrow but continuous field

of solid solutions in the quaternary iron-chromium-nickel-molybdenum system, extending from the iron-nickel-molybdenum P to the chromium-nickel-molybdenum P phase. Such quaternary alloys have not been investigated in the present work.

It was reported previously (reference 10) that various intermediate phases such as  $\mu$  and  $\sigma$ , in binary and ternary alloys of the transition elements, may be ascribed rather characteristic ranges of electron vacancy concentration in the 3d sub-band. The electron vacancy concentration  $N_v$  for single-phase alloys was calculated from the  $N_v$  values of the components on the assumption of simple additivity, according to:

$$N_v = 4.66(\text{Cr} + \text{Mo}) + 2.66(\text{Fe}) + 1.71(\text{Co}) + 0.61(\text{Ni}) \quad (1)$$

or

$$N_v = 5.6(\text{Mo}) + 4.66(\text{Cr}) + 2.66(\text{Fe}) + 1.71(\text{Co}) + 0.61(\text{Ni}) \quad (2)$$

where the chemical symbols stand for the atomic fractions of the corresponding metals in the alloy and the numerical coefficients are the  $N_v$  values for the elements, as given by Pauling in reference 12 (except for molybdenum). Equation (1) is based on the assumption that the number of electron vacancies contributed to the alloy by the 4d sub-band of molybdenum is the same as that contributed by the 3d sub-band of chromium, namely, 4.66. In the previous work (reference 10), better alinement of the  $\sigma$  phase fields in the cobalt-chromium-molybdenum and nickel-chromium-molybdenum systems with the lines of constant electron vacancy concentration was obtained by ascribing to molybdenum an electron vacancy number of 5.6, as in equation (2). In the following paragraphs the electron vacancy considerations are applied to the intermediate phases in the ternary systems investigated in the present work.

The  $\sigma$  phase was reported by Goldschmidt to occur at high temperatures in both the cobalt-molybdenum (reference 13) and the iron-molybdenum (reference 11) systems. Assuming that the cobalt-molybdenum  $\sigma$  is identical with the  $\eta$  phase of Sykes and Graff (reference 6) and that the iron-molybdenum  $\sigma$  is identical with  $\zeta$  in the current iron-molybdenum phase diagram (reference 4), the  $N_v$  values can be calculated and compared with those obtained for  $\sigma$  in other systems. The  $N_v$  values obtained from equation (2), namely, 4.10 and 4.13, respectively, are much higher than the average of 3.4 to 3.5 for  $\sigma$  in other systems. However, equation (1) gives  $N_v = 3.52$  for the cobalt-molybdenum  $\sigma$  and  $N_v = 3.66$  for the iron-molybdenum  $\sigma$ . The latter can be brought into still better agreement with the usual



range, if an  $N_v$  value of 2.22 is accepted for iron, corresponding to magnetic saturation measurements, instead of  $N_v = 2.66$ , as given by Pauling (reference 12). This gives  $N_v = 3.44$  for the iron-molybdenum sigma. Figure 23 shows "equivacancy" lines for the cobalt-iron-molybdenum system, drawn on the basis of the above values for molybdenum and iron. It is seen that both the dash-dot line connecting the two binary sigma compositions (presumably representing the sigma solid-solution field which may exist above about 1250° C) and the mu phase field are reasonably well aligned with these equivacancy lines.

In the cobalt-nickel-molybdenum and iron-nickel-molybdenum systems the elongated mu phase fields give very poor alignment with the equivacancy lines drawn according to either equation (1) or equation (2). Good alignment can be obtained with equation (1), if the  $N_v$  value for nickel is changed from 0.61 to about 1.6, as shown in figures 24 and 25. The selection of this value for the sake of these two phase diagrams alone might be considered unjustified, particularly since the saturation value of the magnetic moment corresponds to 0.61. However, it appears that with  $N_v = 1.6$  the alignment of the sigma phase in the cobalt-nickel-chromium system (reference 10) is also considerably improved (fig. 26). Furthermore, with the  $N_v$  value of 1.6 for nickel, the composition range of the vanadium-nickel sigma phase, 55 to 65 atomic percent vanadium, as determined by Pearson, Christian, and Hume-Rothery (reference 14), gives an  $N_v$  range of 3.28 to 3.59, which is in good agreement with that for other sigma phases. It was reported previously (reference 10) that the electron vacancy concentration for this phase, calculated with  $N_v = 0.61$  for nickel, was unaccountably low. An interesting corollary of these findings is the fact that the magnetic moment for nickel in the paramagnetic condition, as calculated from the Curie constant, is reported to be 1.6 Bohr magnetons per atom (reference 15), in agreement with the value deduced above.

## CONCLUSIONS

A survey at 1200° C of portions of the iron-nickel-molybdenum and cobalt-iron-molybdenum ternary systems indicated the following conclusions:

1. The 1200° C isothermal section of the cobalt-iron-molybdenum ternary system was investigated up to 62 percent molybdenum by means of X-ray diffraction and microscopic methods, using 57 vacuum-melted alloys. The face-centered cubic alpha solid solutions, based on the austenitic iron-cobalt binary phase, dissolve up to 22.5 percent molybdenum near

the cobalt corner. The solubility of molybdenum decreases to about 2 percent near the iron corner. Near the iron corner the alpha phase transforms to epsilon upon quenching from 1200° C to room temperature.

The body-centered cubic epsilon phase, based on the binary iron-molybdenum ferrite, extends in the form of a triangular field to 21 percent cobalt and 19 percent molybdenum. The isomorphous binary intermediate phases cobalt-molybdenum mu and iron-molybdenum mu form uninterrupted solid solutions. The elongated mu phase field extends roughly parallel to the iron-cobalt side of the diagram. The alpha, epsilon, and mu phases coexist with each other in three two-phase fields and in a very narrow three-phase field.

2. The 1200° C isothermal section of the iron-nickel-molybdenum ternary system was investigated up to 64.5 percent molybdenum by means of X-ray diffraction and microscopic methods using 105 vacuum-melted alloys. The face-centered cubic alpha phase field, based on the austenitic iron-nickel binary solid solutions, takes into solution up to 35.5 percent molybdenum near the nickel corner. The solubility of molybdenum decreases to 2 percent near the iron corner. In this area the austenite transforms into ferrite upon quenching from 1200° C to room temperature.

The body-centered cubic epsilon phase, based on binary iron-molybdenum ferrite, occupies a triangular field to the corner approximately corresponding to 8 percent nickel and 21 percent molybdenum. The mu phase field extends in the form of a narrow strip, roughly parallel to the iron-nickel side of the diagram, up to 19.4 percent nickel. The delta field, based on the nickel-molybdenum intermediate phase, extends to 8.5 percent iron. Between these two phases the ternary P phase occupies a small range of compositions. The three phases mu, P, and delta occupy a narrow strip, only slightly inclined with respect to the iron-nickel side of the diagram. The following three-phase fields exist: (1) Alpha, epsilon, and mu, (2) alpha, mu, and P, and (3) alpha, P, and delta. The two-phase fields in the investigated portion of the diagram are as follows: (a) Alpha and epsilon, (b) alpha and mu, (c) mu and epsilon, (d) alpha and P, (e) mu and P, (f) delta and alpha, and (g) P and delta.

University of Notre Dame

Notre Dame, Ind., January 1, 1952

## REFERENCES

1. Manly, W. D., and Beck, Paul A.: Survey of the Chromium-Cobalt-Nickel Phase Diagram at 1200° C. NACA TN 2602, 1952.
2. Kamen, E. L., and Beck, Paul A.: Survey of Portions of the Cobalt-Chromium-Iron-Nickel Quaternary System. NACA TN 2603, 1952.
3. Rideout, Sheldon Paul, and Beck, Paul A.: Survey of Portions of the Chromium-Cobalt-Nickel-Molybdenum Quaternary System at 1200° C. NACA TN 2683, 1952.
4. Lyman, Taylor, ed.: Metals Handbook. Am. Soc. Metals (Cleveland), 1948.
5. Henglein, E., and Kohsok, H.: La détermination de la phase  $\text{Co}^7\text{Mo}^6$ . Rev. metallurgie, vol. 46, no. 9, Sept. 1949, pp. 569-571.
6. Sykes, W. P., and Graff, H. F.: The Cobalt-Molybdenum System. Trans. Am. Soc. Metals, vol. 23, 1935, p. 249.
7. Ellis, W. C., and Greiner, E. S.: Equilibrium Relations in the Solid State of the Iron-Cobalt System. Trans. Am. Soc. Metals, vol. 29, 1941, pp. 415-431.
8. Köster, V. W.: Das System Eisen-Nickel-Molybdän. Archiv Eisenhüttenwesen, Bd. 8, 1934, p. 169.
9. Köster, W., and Tonn, W.: Das System Eisen-Kobalt-Molybdän. Archiv Eisenhüttenwesen, Bd. 5, 1932, p. 627.
10. Rideout, Sheldon P., Manly, W. D., Kamen, E. L., Lement, B. S., and Beck, P. A.: Intermediate Phases in Ternary Alloy Systems of Transition Elements. Jour. Metals, vol. 3, no. 10, Oct. 1951, pp. 872-876.
11. Goldschmidt, H. J.: A Molybdenum Sigma Phase. Research, vol. 2, no. 7, July 1949, pp. 343-344.
12. Pauling, L.: The Nature of the Interatomic Forces in Metals. Phys. Rev., vol. 54, no. 11, second ser., Dec. 1, 1938, pp. 899-904.
13. Goldschmidt, H. J.: Phase Diagrams of the Ternary Systems Fe-Cr-W and Fe-Cr-Mo at Low Temperatures. Symposium on High Temperature Steels and Alloys for Gas Turbines. The Iron and Steel Inst. (London), 1951, pp. 249-257.

14. Pearson, W. B., Christian, J. W., and Hume-Rothery, W.: New Sigma Phases in Binary Alloys of the Transition Elements of the First Long Period. *Nature*, vol. 167, 1951, p. 110.
15. Bozorth, R. M.: Magnetism. *Rev. Modern Phys.*, vol. 19, no. 1, Jan. 1947, pp. 29-86.

TABLE I

LOT ANALYSES IN WEIGHT PERCENT OF METALS USED  
FOR PREPARING ALLOYS

Element or compound	Cobalt rondelles	Molybdenum rod	Electrolytic -	
			Iron	Nickel
C	0.17	0.003	0.010	-----
CaO	.12	-----	-----	-----
Co	Bal.	-----	-----	0.6 to 0.8
Cr	-----	-----	<.015	-----
Cu	.02	-----	<.03	.01
Fe	.12	.005	Bal.	.01
H <sub>2</sub>	-----	-----	-----	-----
MgO	.04	-----	-----	-----
Mn	.06	-----	.01	-----
Mo	-----	Bal.	.015	-----
Ni	.46	-----	<.03	Bal.
O <sub>2</sub>	-----	.003	-----	-----
P	-----	-----	.003	-----
S	.009	-----	.002	.001
SiO <sub>2</sub>	.13	-----	.03	-----



TABLE II

## CRUCIBLES USED FOR MELTING VARIOUS ALLOYS

Stabilized zirconia	Alundum	Recrystallized alumina
801 to 819	647 to 649 658 to 660 784 to 800	693 to 695 698 to 706 709 to 713 716 to 783 820 to 864



TABLE III

## MICROSCOPIC AND X-RAY DATA FOR COBALT-IRON-MOLYBDENUM ALLOYS

[Data for figs. 8 and 9]

Alloy	Composition (weight percent)			Estimated amounts of phases (percent)				X-ray	Annealing time <sup>a</sup> at 1200° C (hr)
	Co	Fe	Mo	Alpha	Epsilon	Mu	Second phase		
Alpha alloys									
432	79.0	0	21.0	100	0	0	0	Alpha	48
693	19.8	70.0	10.2	100	0	0	0	Epsilon	48
742	26.0	64.0	10.0	100	0	0	0	Epsilon	48
743	34.0	56.0	10.0	100	0	0	0	Epsilon	48
789	36.0	56.0	8.0	100	0	0	0	Epsilon	48
790	38.0	56.0	6.0	100	0	0	0	Epsilon	48
791	56.0	28.0	16.0	100	0	0	0	Alpha	48
792	66.0	16.0	18.0	100	0	0	0	Alpha	48
799	39.0	45.0	16.0	100	0	0	0	Alpha and epsilon	48
800	44.0	40.0	16.0	100	0	0	0	Alpha and epsilon	48
<sup>b</sup> 822	19.10	70.44	10.46	100	0	0	0	Epsilon	48
<sup>b</sup> 834	0	98.75	1.25	100	0	0	0	Epsilon	48
Epsilon alloys									
<sup>b</sup> 694	16.56	70.34	13.10	0	100	0	0	Epsilon	48
<sup>b</sup> 788	0	80.16	19.84	0	100	0	0	Epsilon	48
<sup>b</sup> 835	0	95.14	4.86	0	100	0	0	Epsilon	48
<sup>b</sup> 841	19.87	62.39	17.74	0	100	0	0	Epsilon	48
Alpha-plus-epsilon alloys									
820	17.2	70.0	12.8	20	80	0	0	Epsilon	48
821	18.0	70.0	12.0	80	20	0	0	Epsilon	48
<sup>b</sup> 842	23.05	60.52	16.43	75	25	0	0	Epsilon	48
Mu alloys									
610	0	46.6	53.4	0	0	100	0	Mu	96
637	10.0	54.0	36.0	0	0	100	0	Mu	96
638	18.0	25.0	57.0	0	0	100	0	Mu	96
639	30.0	11.5	58.5	0	0	100	0	Mu	96
795	11.0	36.5	52.5	0	0	100	0	Mu	96
796	9.4	35.1	55.5	0	0	100	0	Mu	96
797	21.0	26.0	53.0	0	0	100	0	Mu	96
798	33.2	12.4	54.4	0	0	100	0	Mu	96
830	45.0	0	55.0	0	0	100	0	Mu	96
843	0	44.0	56.0	0	0	100	0	Mu	96

<sup>a</sup>Alloys forged prior to annealing were homogenized for only 48 hr; the others were annealed for 96 hr.

<sup>b</sup>Composition is by chemical analysis.

NACA

TABLE III.- Concluded

## MICROSCOPIC AND X-RAY DATA FOR COBALT-IRON-MOLYBDENUM ALLOYS - Concluded

Alloy	Composition (weight percent)			Estimated amounts of phases (percent)				X-ray	Annealing time <sup>a</sup> at 1200° C (hr)
	Co	Fe	Mo	Alpha	Epsilon	Mu	Second phase		
Epsilon-plus-mu alloys									
718	10.0	66.0	24.0	0	92	8	0	Epsilon and mu	96
719	15.1	44.9	40.0	0	40	60	0	Epsilon and mu	96
720	14.3	45.7	40.0	0	40	60	0	Epsilon and mu	96
737	6.0	54.0	40.0	0	40	60	0	Epsilon and mu	96
<sup>b</sup> 746	20.17	60.31	19.52	0	99	1	0	Epsilon	96
<sup>b</sup> 826	10.17	70.24	19.59	0	99.5	.5	0	Epsilon	48
<sup>b</sup> 829	0	78.19	21.81	0	99	1	0	Epsilon	48
831	10.0	50.0	40.0	0	40	60	0	Epsilon and mu	96
832	12.5	47.5	40.0	0	40	60	0	Epsilon and mu	96
<sup>b</sup> 847	0	48.73	51.27	0	2	98	0	Mu	96
Alpha-plus-mu alloys									
<sup>b</sup> 399	77.08	0	22.92	98	0	2	0	Alpha	48
695	54.0	26.0	20.0	97	0	3	0	Alpha	48
716	26.0	48.0	26.0	80	0	20	0	Epsilon and mu	96
738	26.0	30.0	44.0	20	0	80	0	Epsilon and mu	96
739	40.0	14.0	46.0	18	0	82	0	Alpha and mu	96
744	40.0	40.0	20.0	96	0	4	0	Alpha and epsilon	48
745	47.0	33.0	20.0	97	0	3	0	Alpha	48
747	23.1	50.3	26.6	80	0	20	0	Epsilon and mu	96
748	31.0	24.0	45.0	18	0	82	0	Alpha and mu	96
749	35.0	19.0	46.0	18	0	82	0	Alpha and mu	96
793	28.0	28.0	44.0	20	0	80	0	Alpha and mu	96
794	30.0	26.0	44.0	20	0	80	0	Alpha, epsilon, and mu	96
<sup>b</sup> 823	38.76	43.26	17.98	99.5	0	.5	0	Alpha and epsilon	48
<sup>b</sup> 824	53.88	28.20	17.92	100	0	Trace	0	Alpha	48
<sup>b</sup> 825	63.95	16.22	19.83	100	0	Trace	0	Alpha	48
<sup>b</sup> 828	25.01	56.32	18.67	97	0	3	0	Epsilon	48
849	22.0	27.0	51.0	2	0	98	0	Mu	96
850	33.0	15.0	52.0	2	0	98	0	Mu	96
<sup>b</sup> 851	47.18	0	52.82	3	0	97	0	Mu	96
853	23.5	40.5	36.0	45	0	55	0	Epsilon and mu	96
Alpha-plus-epsilon-plus-mu alloys									
<sup>b</sup> 717	20.81	51.89	27.34	10	70	20	0	Epsilon and mu	96
827	22.0	59.0	19.0	29	59	2	0	Epsilon	48
852	21.0	43.0	36.0	30	15	55	0	Epsilon and mu	96
Mu and second phase of higher Mo									
<sup>b</sup> 611	38.33	0	61.67	0	0	98	2	Mu	96
845	25.0	15.0	60.0	0	0	99	1	Mu	96
<sup>b</sup> 848	0	42.15	57.85	0	0	98	2	Mu	96

<sup>a</sup>Alloys forged prior to annealing were homogenized for only 48 hr; the others were annealed for 96 hr.

<sup>b</sup>Composition is by chemical analysis.

NACA



TABLE IV

## MICROSCOPIC AND X-RAY DATA FOR IRON-NICKEL-MOLYBDENUM ALLOYS

[Data for figs. 10 and 11]

Alloy	Composition (weight percent)			Estimated amounts of phases (percent)						X-ray	Annealing time <sup>a</sup> at 1200° C (hr)	
	Fe	Ni	Mo	Alpha	Epsilon	Mu	P	Delta	Second phase			
Alpha alloys												
400	0	65.0	35.0	100	0	0	0	0	0	Alpha	48	
700	55.0	29.0	16.0	100	0	0	0	0	0	Alpha	48	
b770	90.20	4.08	5.72	100	0	0	0	0	0	Epsilon	48	
b773	79.93	8.60	11.47	100	0	0	0	0	0	Epsilon	48	
b779	20.17	55.12	24.71	100	0	0	0	0	0	Alpha	48	
801	90.0	6.0	4.0	100	0	0	0	0	0	Epsilon	48	
802	80.0	11.0	9.0	100	0	0	0	0	0	Epsilon	48	
814	25.0	51.0	24.0	100	0	0	0	0	0	Alpha	48	
815	9.5	61.0	29.5	100	0	0	0	0	0	Alpha	48	
b834	98.75	0	1.25	100	0	0	0	0	0	Epsilon	48	
839	25.0	50.0	25.0	100	0	0	0	0	0	Alpha	48	
840	16.1	56.5	27.4	100	0	0	0	0	0	Alpha	48	
Epsilon alloys												
721	78.0	6.0	16.0	0	100	0	0	0	0	Epsilon	48	
b768	90.19	2.01	7.80	0	100	0	0	0	0	Epsilon	48	
b788	80.16	0	19.84	0	100	0	0	0	0	Epsilon	48	
b835	95.14	0	4.86	0	100	0	0	0	0	Epsilon	48	
836	75.5	7.0	17.5	0	100	0	0	0	0	Epsilon	48	
837	74.0	7.0	19.0	0	100	0	0	0	0	Epsilon	48	
854	72.5	7.0	20.5	0	100	0	0	0	0	Epsilon	48	
Mu alloys												
610	46.6	0	53.4	0	0	100	0	0	0	Mu	96	
b648	34.69	9.89	55.42	0	0	100	0	0	0	Mu	96	
b660	27.94	15.08	56.98	0	0	100	0	0	0	Mu	96	
b709	30.82	12.95	56.23	0	0	100	0	0	0	Mu	96	
b710	24.79	17.15	58.06	0	0	100	0	0	0	Mu	96	
784	40.5	5.0	54.5	0	0	100	0	0	0	Mu	96	
b785	32.16	10.12	57.72	0	0	100	0	0	0	Mu	96	
819	40.5	5.5	54.0	0	0	100	0	0	0	Mu	96	
843	44.0	0	56.0	0	0	100	0	0	0	Mu	96	
858	25.5	15.0	59.5	0	0	100	0	0	0	Mu	96	
859	24.5	15.0	60.5	0	0	100	0	0	0	Mu	96	
Alpha-plus-epsilon alloys												
b698	74.12	10.07	15.71	70	30	0	0	0	0	Epsilon	48	
b769	90.63	3.09	6.28	60	40	0	0	0	0	Epsilon	48	
b771	80.58	7.16	12.26	40	60	0	0	0	0	Epsilon	48	
b772	79.96	8.13	11.91	95	5	0	0	0	0	Epsilon	48	
b816	79.65	6.64	13.71	15	85	0	0	0	0	Epsilon	48	
817	76.0	8.0	16.0	20	80	0	0	0	0	Epsilon	48	
818	75.0	9.0	16.0	50	50	0	0	0	0	Epsilon	48	
b838	73.01	11.04	15.95	90	10	0	0	0	0	Epsilon	48	
855	72.0	8.5	19.5	10	90	0	0	0	0	Epsilon	48	

<sup>a</sup>Alloys forged prior to annealing were homogenized for only 48 hr; the others were annealed for 96 hr.

<sup>b</sup>Composition is by chemical analysis.



TABLE IV.- Continued

## MICROSCOPIC AND X-RAY DATA FOR IRON-NICKEL-MOLYBDENUM ALLOYS - Continued

Alloy	Composition (weight percent)			Estimated amounts of phases (percent)						X-ray	Annealing time <sup>a</sup> at 1200° C (hr)
	Fe	Ni	Mo	Alpha	Epsilon	Mu	P	Delta	Second phase		
Alpha-plus-mu alloys											
b699	66.04	18.06	15.90	98	0	2	0	0	0	Alpha	48
b701	31.85	44.83	23.32	98	0	2	0	0	0	Alpha	48
702	45.0	17.0	38.0	50	0	50	0	0	0	Alpha and mu	96
703	36.0	26.0	38.0	50	0	50	0	0	0	Alpha and mu	96
704	27.0	34.0	39.0	50	0	50	0	0	0	Alpha and mu	96
b722	71.75	12.07	16.18	98	0	2	0	0	0	Alpha and epsilon	48
b723	69.78	14.19	16.03	97	0	3	0	0	0	Alpha and epsilon	48
b724	67.87	16.21	15.92	97	0	3	0	0	0	Alpha	48
725	55.0	26.0	19.0	92	0	8	0	0	0	Alpha	48
b726	20.13	52.89	26.98	100	0	Trace	0	0	0	Alpha	48
729	51.0	11.0	38.0	45	0	65	0	0	0	Alpha and mu	96
730	39.0	11.0	50.0	10	0	90	0	0	0	Alpha and mu	96
b756	24.89	32.02	43.09	40	0	60	0	0	0	Alpha and mu	96
757	23.0	30.0	47.0	30	0	70	0	0	0	Alpha and mu	96
763	34.0	24.0	42.0	35	0	65	0	0	0	Alpha and mu	96
764	32.0	21.0	47.0	25	0	75	0	0	0	Alpha and mu	96
765	43.0	16.0	41.0	35	0	65	0	0	0	Alpha and mu	96
766	40.0	15.0	45.0	25	0	75	0	0	0	Alpha and mu	96
767	37.5	12.5	50.0	12	0	88	0	0	0	Alpha and mu	96
774	53.0	9.0	38.0	40	0	60	0	0	0	Alpha and mu	96
776	47.0	8.0	45.0	20	0	80	0	0	0	Alpha and mu	96
b777	49.23	6.11	44.66	20	0	80	0	0	0	Alpha and mu	96
b778	55.15	27.61	17.24	99	0	1	0	0	0	Alpha	48
780	23.0	42.0	35.0	70	0	30	0	0	0	Alpha and mu	96
b782	24.07	19.92	56.01	5	0	95	0	0	0	Mu	96
b805	35.54	11.39	53.07	2	0	98	0	0	0	Mu	96
b812	25.62	18.11	56.27	3	0	97	0	0	0	Mu	96
b813	43.54	36.25	20.21	99	0	1	0	0	0	Alpha	48
857	20.0	39.0	41.0	55	0	45	0	0	0	Alpha and mu	96
862	42.5	5.0	52.5	4	0	96	0	0	0	Mu	96
863	23.5	49.5	27.0	94	0	6	0	0	0	Alpha	48
Epsilon-plus-mu alloys											
b728	57.17	5.09	37.74	0	50	50	0	0	0	Epsilon and mu	96
b829	78.19	0	21.81	0	96	4	0	0	0	Epsilon	48
b847	48.73	0	51.27	0	6	94	0	0	0	Mu	96
Alpha-plus-epsilon-plus-mu alloys											
b775	55.10	7.06	37.84	40	10	50	0	0	0	Alpha, epsilon, and mu	96
P alloys											
809	8.5	28.5	63.0	0	0	0	100	0	0	P	96
Alpha-plus-P alloys											
705	15.0	43.0	42.0	40	0	0	60	0	0	Alpha and P	96
754	14.0	41.0	45.0	50	0	0	50	0	0	Alpha and P	96
833	14.7	49.3	36.0	80	0	0	20	0	0	Alpha and P	96
P-plus-mu alloys											
b647	21.92	20.11	57.97	0	0	90	10	0	0	P and mu	96
b786	23.29	18.11	58.60	0	0	92	8	0	0	P and mu	96
b807	14.10	25.63	60.27	0	0	10	90	0	0	P and mu	96
b808	13.07	24.39	62.44	0	0	Trace	100	0	0	P	96

<sup>a</sup>Alloys forged prior to annealing were homogenized for only 48 hr; the others were annealed for 96 hr.<sup>b</sup>Composition is by chemical analysis.

NACA

TABLE IV.- Concluded

## MICROSCOPIC AND X-RAY DATA FOR IRON-NICKEL-MOLYBDENUM ALLOYS - Concluded

Alloy	Composition (weight percent)			Estimated amounts of phases (percent)						X-ray	Annealing time <sup>a</sup> at 1200° C (hr)
	Fe	Ni	Mo	Alpha	Epsilon	Mu	P	Delta	Second phase		
Alpha-plus-P-plus-mu alloys											
b <sub>659</sub>	15.87	24.87	59.26	4	0	26	70	0	0	P and mu	96
b <sub>711</sub>	18.62	22.13	59.25	Trace	0	55	45	0	0	P and mu	96
b <sub>787</sub>	14.39	26.74	58.87	6	0	10	84	0	0	P	96
856	19.0	40.0	41.0	60	0	39	1	0	0	Alpha and mu	96
Delta alloys											
803	0	38.5	61.5	0	0	0	0	100	0	Delta	96
Alpha-plus-delta alloys											
b <sub>486</sub>	0	62.92	37.08	97	0	0	0	3	0	Alpha	48
b <sub>658</sub>	4.96	34.11	60.93	2	0	0	0	98	0	Delta	96
706	8.0	48.0	44.0	60	0	0	0	40	0	Alpha and delta	96
b <sub>712</sub>	6.97	31.84	61.19	2	0	0	0	98	0	Delta	96
b <sub>727</sub>	10.09	59.94	29.97	100	0	0	0	Trace	0	Alpha	48
732	3.0	51.0	46.0	60	0	0	0	40	0	Alpha and delta	96
750	5.0	58.0	37.0	80	0	0	0	20	0	Alpha and delta	96
751	8.0	56.0	36.0	80	0	0	0	20	0	Alpha and delta	96
752	6.5	49.0	44.5	60	0	0	0	40	0	Alpha and delta	96
753	5.0	50.0	45.0	60	0	0	0	40	0	Alpha and delta	96
758	3.0	42.0	55.0	20	0	0	0	80	0	Alpha and delta	96
759	5.0	40.0	55.0	20	0	0	0	80	0	Alpha and delta	96
760	7.0	38.0	55.0	20	0	0	0	80	0	Alpha and delta	96
b <sub>761</sub>	8.04	32.37	59.59	10	0	0	0	90	0	Delta	96
b <sub>781</sub>	14.14	50.22	35.64	75	0	0	0	25	0	Alpha and delta	96
b <sub>844</sub>	0	39.28	60.72	4	0	0	0	96	0	Delta	96
P-plus-delta alloys											
810	7.0	30.0	63.0	0	0	0	20	80	0	P and delta	96
Alpha-plus-P-plus-delta alloys											
b <sub>646</sub>	9.85	29.29	60.86	4	0	0	60	36	0	P and delta	96
b <sub>713</sub>	8.91	31.01	60.08	6	0	0	10	84	0	P and delta	96
b <sub>731</sub>	9.86	34.86	55.28	40	0	0	5	75	0	Delta	96
b <sub>755</sub>	11.94	38.94	49.12	40	0	0	50	10	0	Alpha and P	96
b <sub>762</sub>	10.16	32.25	57.59	10	0	0	60	30	0	P	96
811	10.0	30.0	60.0	5	0	0	90	5	0	P	96
Mu and second phase of higher Mo											
b <sub>806</sub>	30.35	8.82	60.83	0	0	96	0	0	2	Mu	96
b <sub>848</sub>	42.15	0	57.85	0	0	96	0	0	5	Mu	96
P and second phase of higher Mo											
783	12.0	25.0	63.0	0	0	0	99	0	1	P	96
Delta and second phase of higher Mo											
b <sub>804</sub>	0	34.61	65.39	0	0	0	0	98	2	Delta	96
b <sub>846</sub>	5.52	30.81	63.67	0	0	0	0	98	2	Delta	96
P plus delta and second phase of higher Mo											
864	7.5	28.5	64.0	0	0	0	85	10	5	P	96

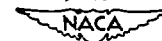
<sup>a</sup>Alloys forged prior to annealing were homogenized for only 48 hr; the others were annealed for 96 hr.<sup>b</sup>Composition is by chemical analysis.

TABLE V

TYPICAL X-RAY DIFFRACTION PATTERN OF FACE-CENTERED CUBIC  
ALPHA PHASE OBTAINED FROM ALLOY 825 WITH  
UNFILTERED CHROMIUM RADIATION

[Co-Fe-Mo system; asymmetric Phragmen focusing camera]

Line	Estimated intensity	$\theta$ (deg)	d (kX)	Radiation Cr K	hkl
1	Strong	29.97	2.0823	Beta	111
2	Very strong	33.25	2.0855	Alpha	111
3	Weak	35.24	1.8030	Beta	200
4	Medium	39.36	1.8030	Alpha	200
5	Weak	54.82	1.2728	Beta	220
6	Medium	63.81	1.2731	Alpha <sub>1</sub>	220
7	Medium	64.03	1.2730	Alpha <sub>2</sub>	220
8	Weak	73.48	1.0851	Beta	311



TABLE VI

TYPICAL X-RAY DIFFRACTION PATTERN OF BODY-CENTERED CUBIC  
EPSILON PHASE OBTAINED FROM ALLOY 768 WITH  
UNFILTERED CHROMIUM RADIATION

[Fe-Ni-Mo system; asymmetric Phragmen focusing camera]

Line	Estimated intensity	$\theta$ (deg)	d (kX)	Radiation Cr K	hkl
1	Strong	30.62	2.0366	Beta	110
2	Very strong	34.19	2.0347	Alpha	110
3	Very weak	46.12	1.4433	Beta	200
4	Medium	52.49	1.4414	Alpha	200
5	Weak	62.19	1.1761	Beta	211
6	Strong	76.31	1.1759	Alpha <sub>1</sub>	211
7	Strong	76.74	1.1757	Alpha <sub>2</sub>	211



TABLE VII

TYPICAL X-RAY DIFFRACTION PATTERN OF MU PHASE OBTAINED FROM  
 ALLOY 784 WITH UNFILTERED CHROMIUM RADIATION  
 [Fe-Ni-Mo system; asymmetric Phragmen focusing camera]

Line	Estimated intensity	$\theta$ (deg)	Line	Estimated intensity	$\theta$ (deg)
1	Medium	25.81	17	Very weak	52.69
2	Strong	28.60	18	Very weak	55.34
3	Very weak	29.03	19	Weak	56.27
4	Weak	29.91	20	Very weak	56.44
5	Very weak	30.31	21	Very weak	58.25
6	Very weak	30.70	22	Weak	59.05
7	Medium	31.52	23	Weak	59.26
8	Very weak	31.91	24	Medium	60.84
9	Weak	32.17	25	Medium	61.03
10	Very weak	32.82	26	Very weak	61.76
11	Very strong	33.25	27	Very weak	61.84
12	Medium	33.72	28	Very weak	64.48
13	Medium	34.15	29	Medium	69.03
14	Very weak	35.55	30	Weak	69.32
15	Weak	36.60	31	Strong	73.85
16	Weak	39.51	32	Medium	74.21

TABLE VIII

TYPICAL X-RAY DIFFRACTION PATTERN OF DELTA PHASE

OBTAINED FROM ALLOY 803

[Fe-Ni-Mo system; asymmetric Phragmen focusing camera]

Line	Estimated intensity	$\theta$ (deg)	Line	Estimated intensity	$\theta$ (deg)
1	Weak	25.17	24	Very weak	54.48
2	Very weak	25.40	25	Very weak	54.78
3	Medium	27.95	26	Very weak	55.45
4	Medium	28.16	27	Very weak	56.04
5	Very weak	28.93	28	Very weak	57.26
6	Weak	29.81	29	Very weak	57.60
7	Medium	30.25	30	Very weak	58.35
8	Weak	30.62	31	Very weak	58.75
9	Strong	31.10	32	Very weak	58.99
10	Weak	31.31	33	Very weak	62.67
11	Weak	31.48	34	Very weak	63.05
12	Medium	32.11	35	Very weak	63.22
13	Very weak	32.46	36	Very weak	63.76
14	Very weak	32.69	37	Very weak	63.98
15	Very weak	32.95	38	Very weak	65.65
16	Strong	33.12	39	Very weak	66.11
17	Very strong	33.68	40	Very weak	66.41
18	Strong	34.05	41	Weak	67.54
19	Medium	35.08	42	Weak	67.76
20	Weak	36.23	43	Weak	70.34
21	Very weak	38.28	44	Weak	70.65
22	Very weak	38.76	45	Weak	77.13
23	Very weak	40.72	46	Weak	77.51

TABLE IX

TYPICAL X-RAY DIFFRACTION PATTERN OF P PHASE  
OBTAINED FROM ALLOY 809

[Fe-Ni-Mo system; asymmetric Phragmen focusing camera]

Line	Estimated intensity	$\theta$ (deg)	Line	Estimated intensity	$\theta$ (deg)
1	Very weak	25.34	28	Weak	36.90
2	Very weak	25.61	29	Very weak	38.43
3	Very weak	26.05	30	Very weak	59.05
4	Very weak	26.38	31	Very weak	59.48
5	Weak	28.22	32	Weak	59.89
6	Medium	28.38	33	Weak	60.08
7	Weak	28.88	34	Weak	61.10
8	Very weak	29.01	35	Weak	61.32
9	Weak	29.19	36	Very weak	62.37
10	Medium	29.48	37	Very weak	62.54
11	Very weak	29.77	38	Very weak	63.26
12	Weak	30.04	39	Very weak	63.49
13	Very weak	30.27	40	Very weak	64.69
14	Weak	30.42	41	Very weak	64.98
15	Medium	30.60	42	Very weak	65.32
16	Strong	31.27	43	Very weak	65.60
17	Weak	32.09	44	Very weak	66.17
18	Very weak	32.53	45	Weak	66.43
19	Strong	32.76	46	Weak	66.97
20	Very weak	33.07	47	Very weak	67.39
21	Strong	33.40	48	Very weak	69.11
22	Weak	33.65	49	Weak	69.49
23	Medium	33.86	50	Weak	72.63
24	Strong	34.05	51	Weak	73.00
25	Very weak	35.05	52	Weak	76.00
26	Weak	36.23	53	Weak	76.41
27	Very weak	36.57			



TABLE X

TYPICAL X-RAY DIFFRACTION PATTERN OF Z PHASE

OBTAINED FROM ALLOY 703

[Fe-Ni-Mo system; asymmetric Phragmen focusing camera]

Line	Estimated intensity	$\theta$ (deg)
1	Very weak	26.84
2	Very weak	27.47
3	Weak	29.29
4	Weak	30.44
5	Strong	32.63
6	Weak	35.72
7	Weak	60.88
8	Weak	61.05



TABLE XI

X-RAY DIFFRACTION DATA AS FUNCTION OF COBALT CONTENT FOR THE  
SATURATED MU PHASE AND DATA FOR A THREE-PHASE ALLOY IN  
THE COBALT-IRON-MOLYBDENUM SYSTEM

[Data for fig. 21]

Alloy	Weight percent cobalt	$\theta$ (deg)	d (kX)
847	0	69.28	1.2215
861	10.0	69.66	1.2184
849	22.0	69.85	1.2170
850	33.0	70.14	1.2148
851	46.0	70.30	1.2135
852	Three-phase alloy	69.78	1.2174



TABLE XII

VARIATION OF LATTICE PARAMETER  $a_0$  OF THE SATURATED ALPHA  
ALLOYS OF THE COBALT-IRON-MOLYBDENUM TERNARY  
SYSTEM AS FUNCTION OF COBALT CONTENT

Alloy	Weight percent cobalt	$a_0$ (KX)
399	77.0	3.5925
825	64.0	3.6005
824	54.0	3.6046
745	47.0	3.6041
800	44.0	3.5995



TABLE XIII

VARIATION OF LATTICE PARAMETER  $a_0$  OF THE SATURATED ALPHA  
PHASE IN THE IRON-NICKEL-MOLYBDENUM TERNARY  
SYSTEM AS FUNCTION OF NICKEL CONTENT

Alloy	Weight percent nickel	$a_0$ (kX)
727	60.0	3.6130
863	49.5	3.6147
726	53.0	3.6187
839	50.0	3.6172
701	45.0	3.6172
813	36.5	3.6146
778	27.5	3.6067
699	18.0	3.6114
724	16.0	3.6135
723	14.0	3.6146



TABLE XIV

X-RAY DIFFRACTION DATA AS FUNCTION OF NICKEL CONTENT  
FOR THE SATURATED MU PHASE IN THE  
IRON-NICKEL-MOLYBDENUM SYSTEM

[Data for fig. 22]

Alloy	Weight percent nickel	$\theta$ (deg)	d (kX)
847	0	69.29	1.2215
862	5.0	69.36	1.2210
805	11.0	69.31	1.2213
812	18.0	69.09	1.2231
782	19.0	69.22	1.2221
647	20.0	69.06	1.2232

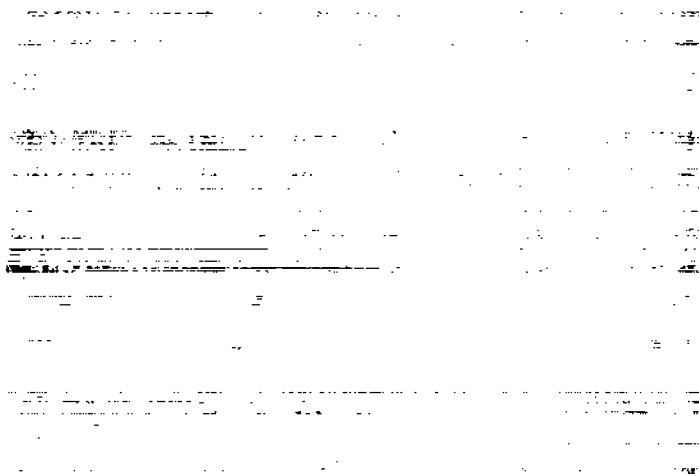


TABLE XV

CORNERS OF THE THREE-PHASE FIELDS OF THE INVESTIGATED  
PORTION OF THE IRON-NICKEL-MOLYBDENUM SYSTEM

Corner	Three-phase field	Composition (weight percent)		
		Fe	Ni	Mo
Alpha	Alpha-mu-epsilon	72.7	11.6	15.7
Epsilon	Alpha-mu-epsilon	71.0	8.0	21.0
Mu	Alpha-mu-epsilon	42.6	4.4	53.0
Alpha	Alpha-mu-P	16.0	55.5	28.5
Mu	Alpha-mu-P	23.3	19.2	57.5
P	Alpha-mu-P	13.3	26.2	60.5
Alpha	Alpha-P-delta	16.0	55.5	28.5
P	Alpha-P-delta	10.0	28.8	61.2
Delta	Alpha-P-delta	8.5	30.0	61.5


 NACA



NACA

Figure 1.- Alloy 844 containing 39.28 percent nickel and 60.72 percent molybdenum. Alpha grains in delta seen in relief; unetched; oblique illumination; X500.

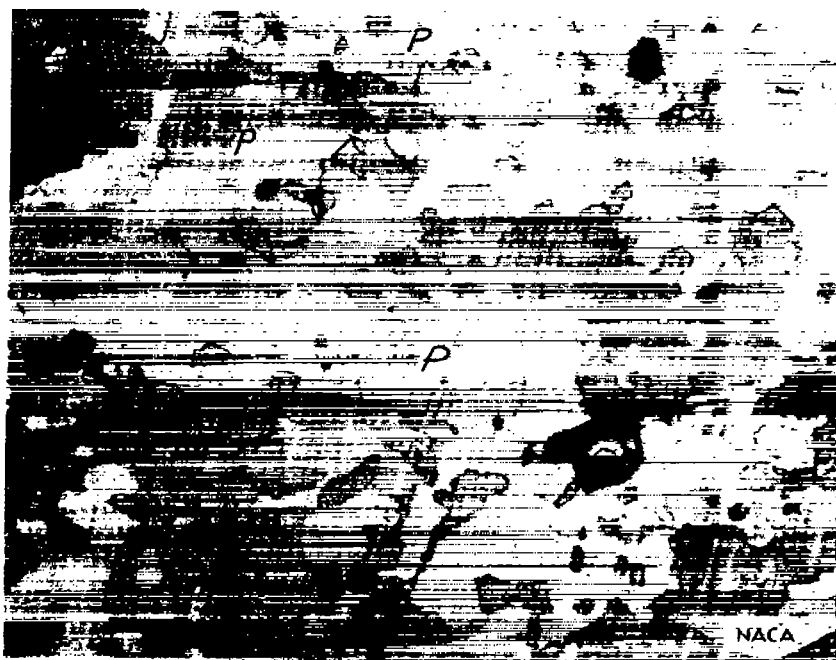


Figure 2.- Alloy 647 containing 21.92 percent iron, 20.11 percent nickel, and 57.97 percent molybdenum. Etched and stained according to procedure 2; P phase stained in brilliant colors, with mu phase stained light to dark tan, depending on orientation; some areas of P marked; X500.



Figure 3.- Alloy 659 containing 15.87 percent iron, 24.87 percent nickel, and 59.26 percent molybdenum. Etched and stained according to procedure 2; light colored mu-phase particles, with dendritic alpha grains embedded in them, in darker matrix of P phase; P phase shows orientation effect; X500.



Figure 4.- Alloy 731 containing 9.86 percent iron, 34.86 percent nickel, and 55.28 percent molybdenum. Etched and stained according to procedure 2; brilliantly colored idiomorphic P-phase particles and slightly roughened alpha grains in matrix of delta phase; stain on delta grains varies slightly with orientation; X500.



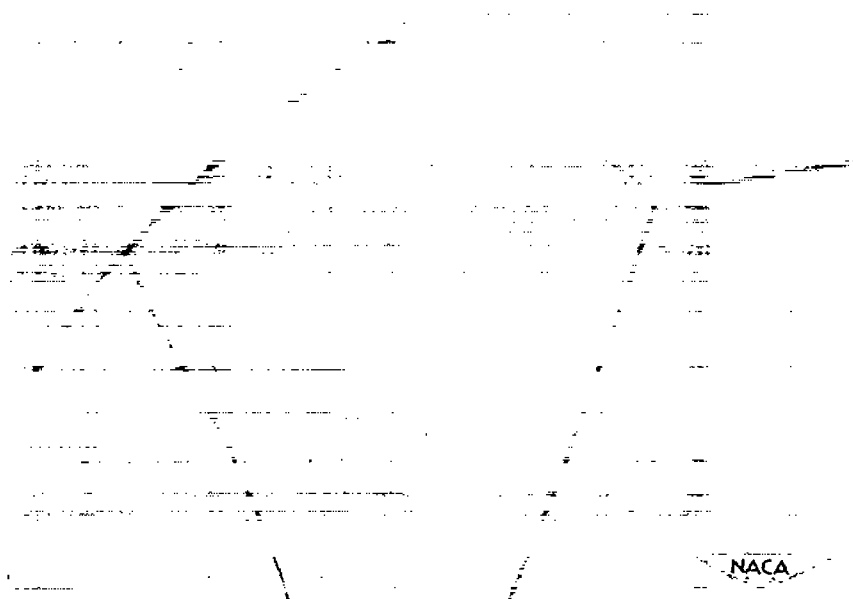


Figure 5.- Alloy 694 containing 16.56 percent cobalt, 70.34 percent iron, and 13.10 percent molybdenum. Etched according to procedure 1; 100-percent-epsilon phase, with very large grains; X100.



Figure 6.- Alloy 746 containing 20.17 percent cobalt, 60.31 percent iron, and 19.52 percent molybdenum. Etched according to procedure 1; white grains of mu phase in matrix of epsilon along epsilon grain boundaries; epsilon phase stains to a very dark color in this region of the ternary diagram; grain boundaries of epsilon phase revealed; X500.

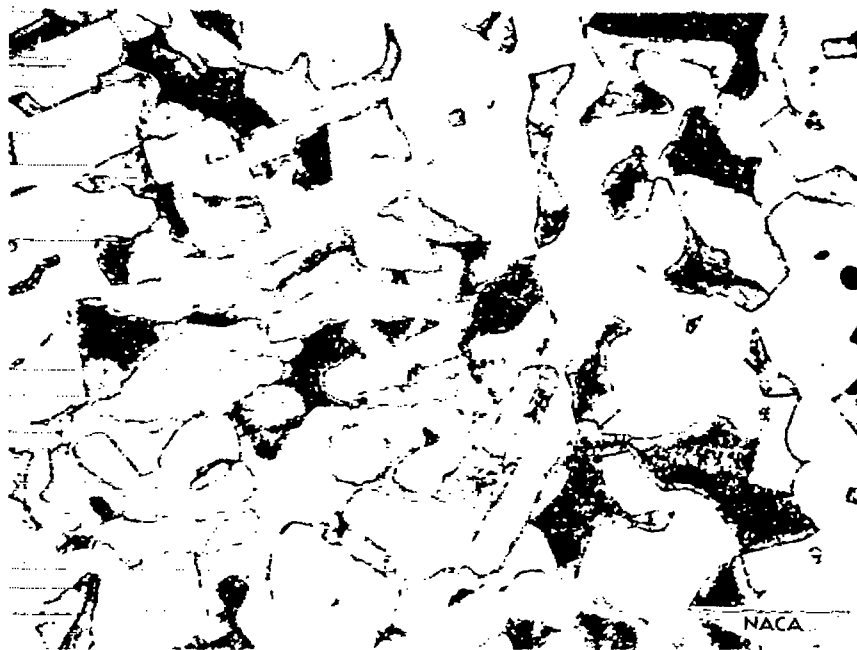


Figure 7.- Alloy 852 containing 21.0 percent cobalt, 43.0 percent iron, and 36.0 percent molybdenum. Etched according to procedure 1; three-phase alloy of alpha, showing roughened grains, unattacked mu, and dark epsilon; X500.

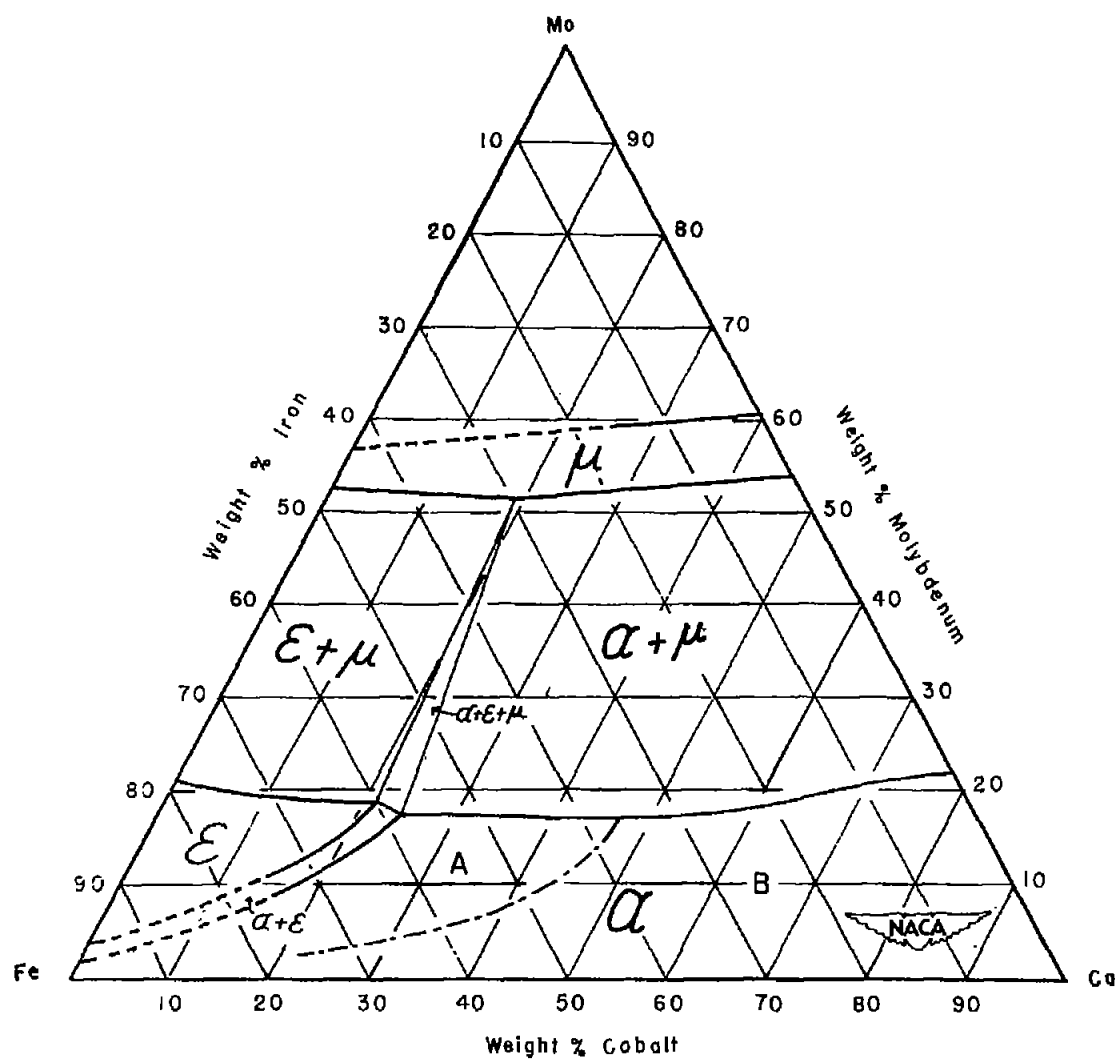


Figure 8.- The 1200° C isothermal section of the cobalt-iron-molybdenum ternary system.

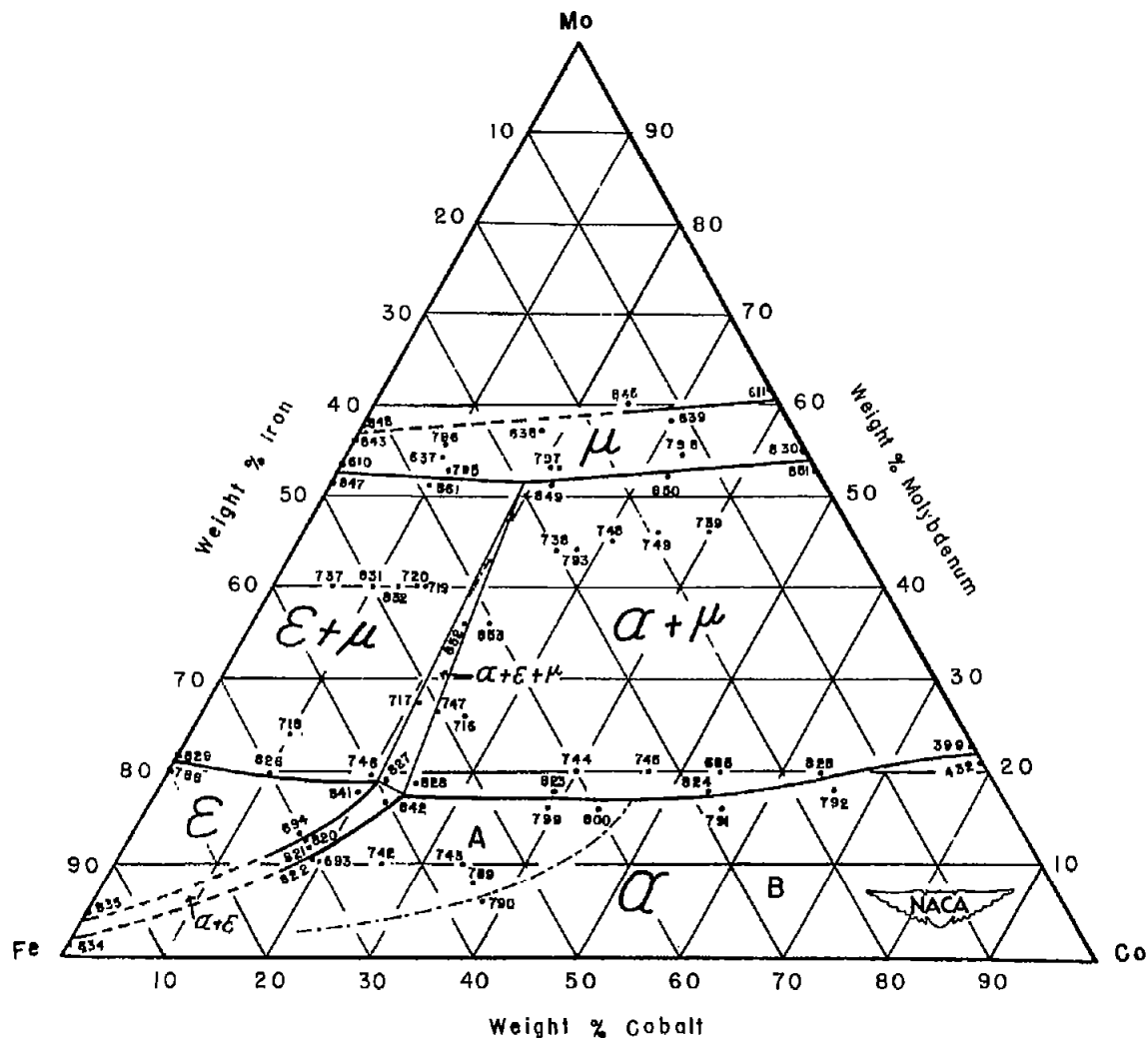


Figure 9.- The 1200° C isothermal section of the cobalt-iron-molybdenum ternary system with alloy compositions indicated.

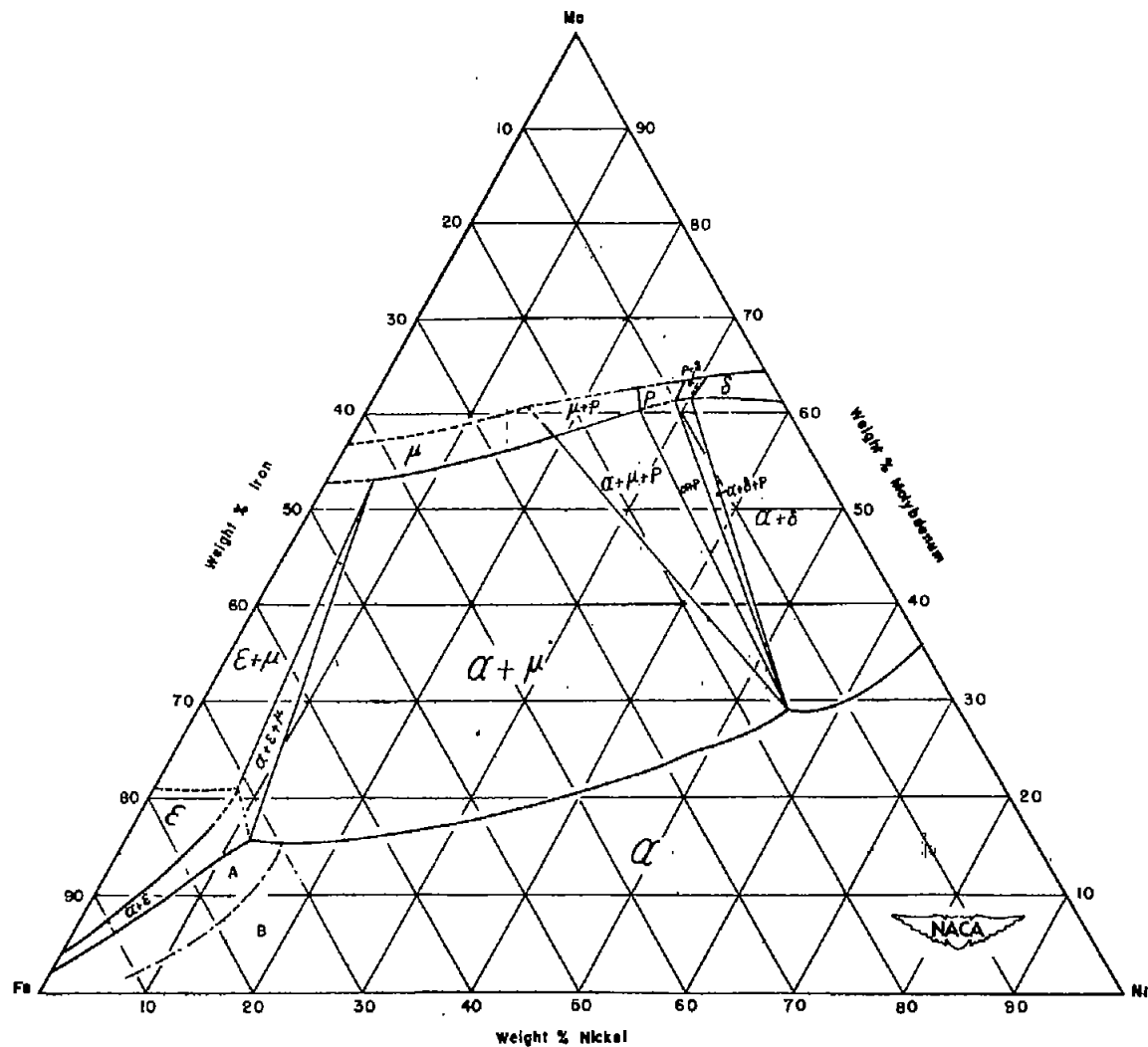


Figure 10.- The 1200° C isothermal section of the iron-nickel-molybdenum ternary system.

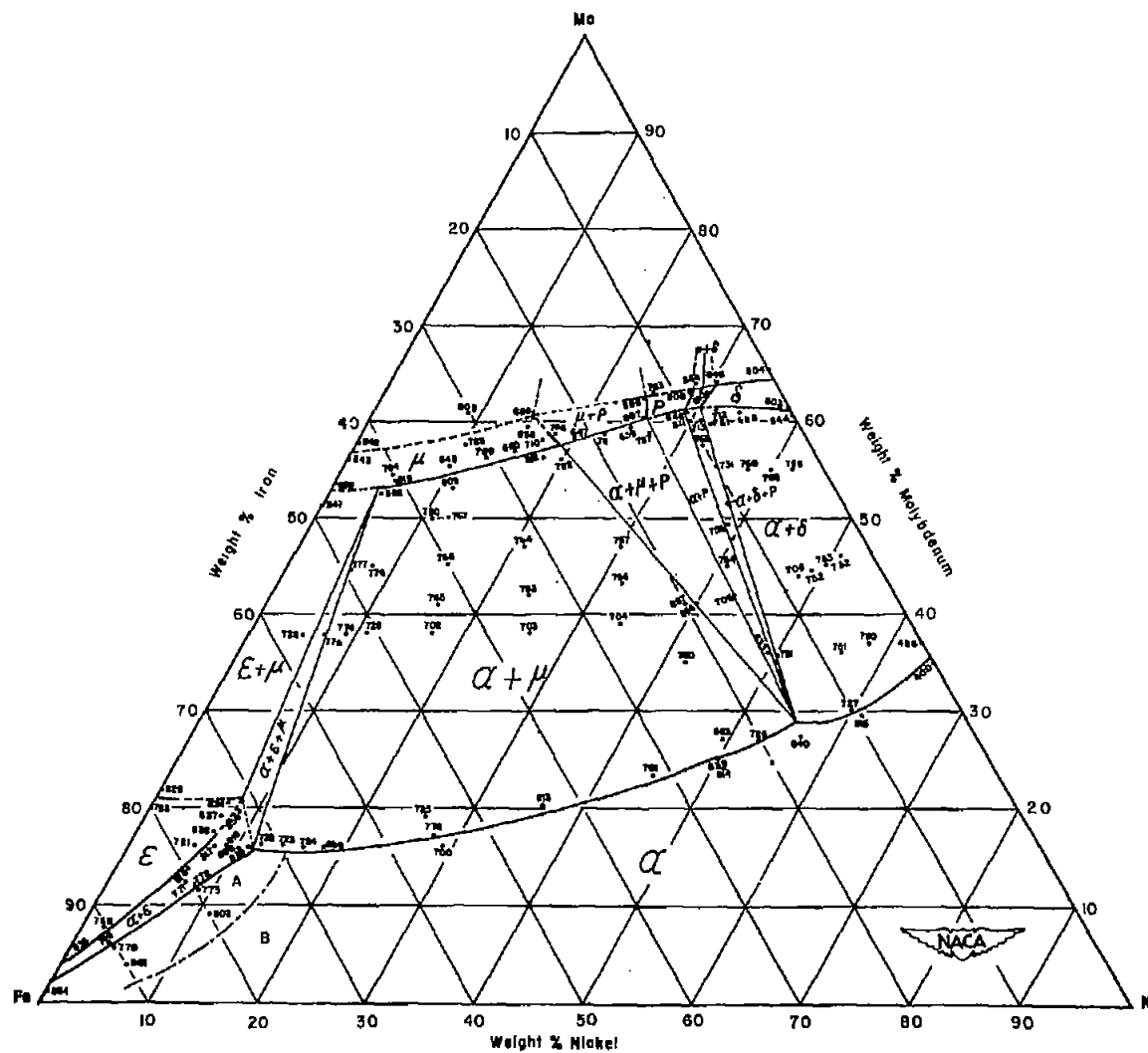


Figure 11.- The 1200° C isothermal section of the iron-nickel-molybdenum ternary system with alloy compositions indicated.

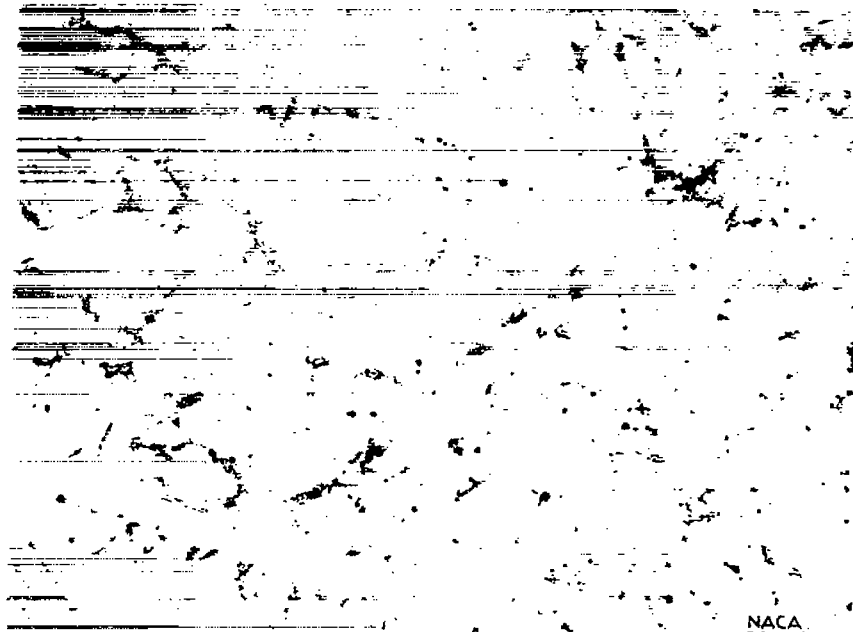


Figure 12.- Alloy 701 containing 31.85 percent iron, 44.83 percent nickel, and 23.32 percent molybdenum. Etched according to procedure 1; typical structure of alpha phase, with fairly large grains and showing annealing twins; second phase mu is not clearly distinguishable because of low magnification; X50.



Figure 13.- Alloy 743 containing 34.0 percent cobalt, 56.0 percent iron, and 10.0 percent molybdenum. Etched according to procedure 1; typical structure of transformed alpha; X50.

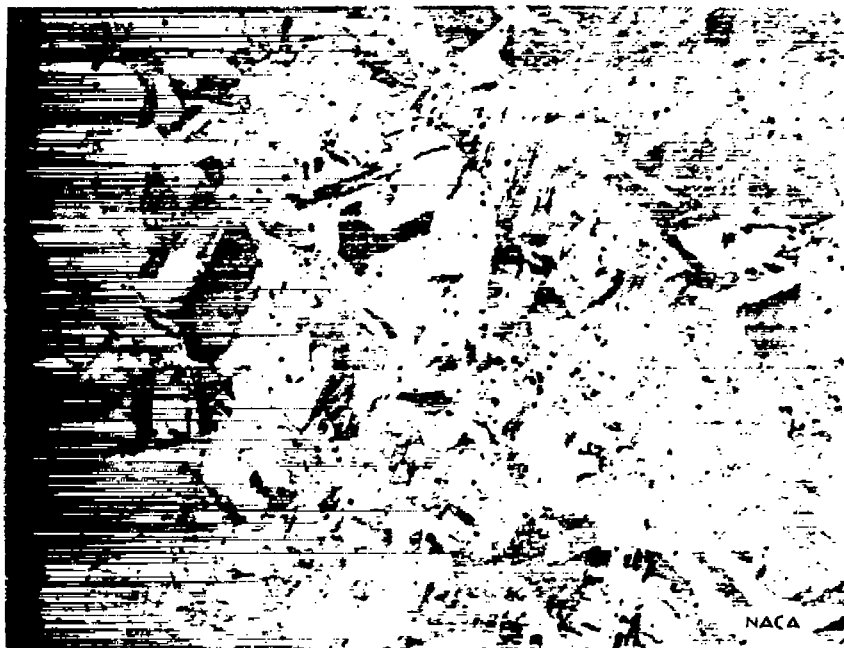


Figure 14.- Alloy 693 containing 19.8 percent cobalt, 70.0 percent iron, and 10.2 percent molybdenum. Completely transformed alpha, with no epsilon phase present; large grain size resulting from grain growth in alloy consisting of a single phase at annealing temperature; X50.

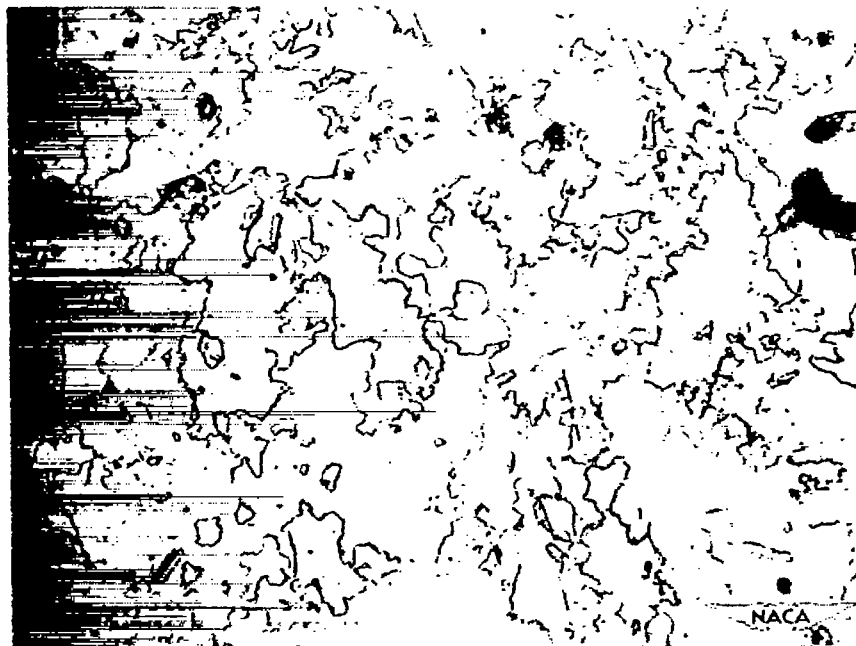


Figure 15.- Alloy 648 containing 34.69 percent iron, 9.89 percent nickel, and 55.42 percent molybdenum. Etched and stained according to procedure 2; a light tan stain throughout; typical structure of mu phase; X500.



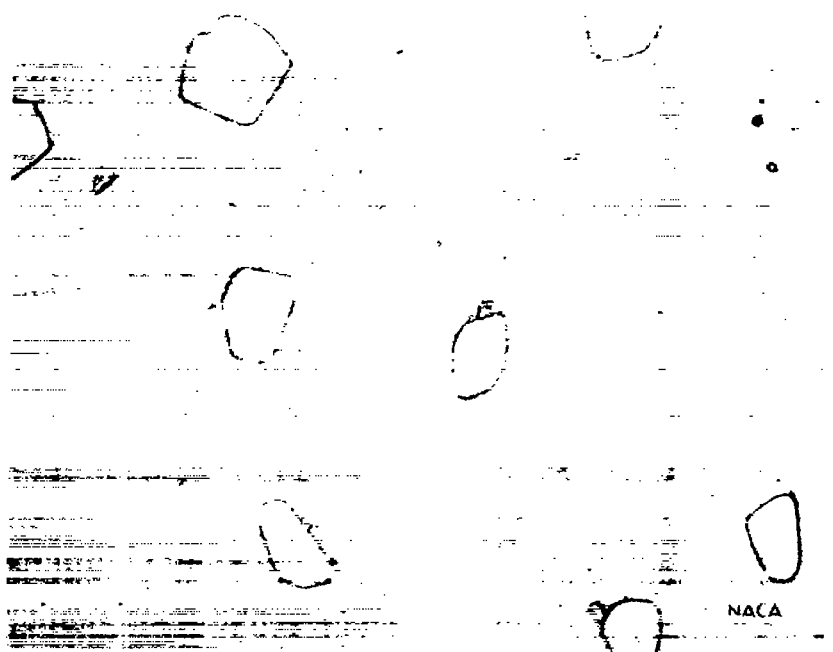


Figure 16.- Alloy 829 containing 78.19 percent iron, 0 percent nickel, and 21.81 percent molybdenum. Etched lightly according to procedure 1; mu phase grains clearly delineated in matrix of epsilon; etching was too light to reveal grain boundaries of epsilon phase; X500.

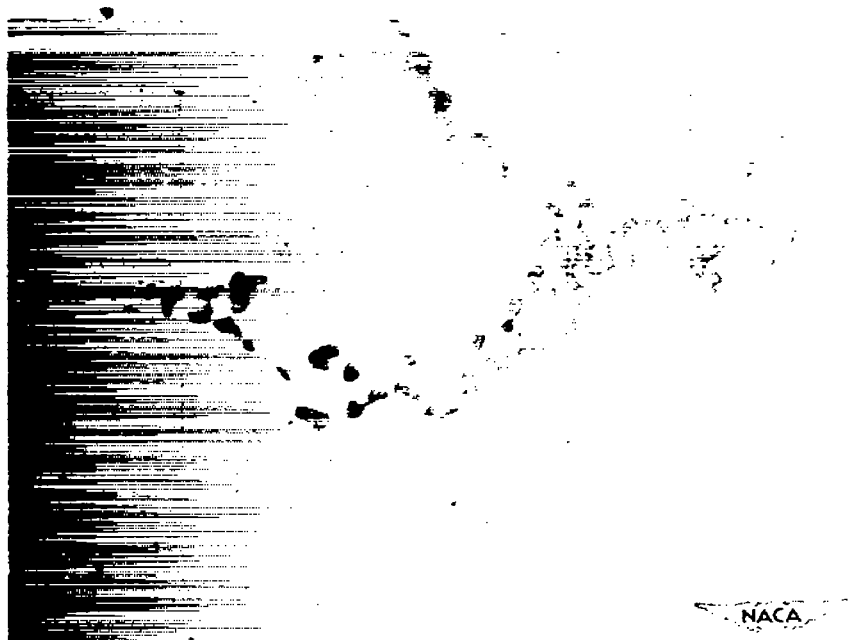


Figure 17.- Alloy 725 containing 55.0 percent iron, 26.0 percent nickel, and 19.0 percent molybdenum. Lightly etched and stained according to procedure 2; stained particles of  $\mu$  phase in matrix of  $\alpha$ ; X500.



Figure 18.- Alloy 762 containing 10.16 percent iron, 32.25 percent nickel, and 57.59 percent molybdenum. Etched and stained according to procedure 2; slightly lighter delta grains and dendritic roughened alpha in matrix of P phase, which shows an orientation effect; some areas of delta phase marked; X500.



Figure 19.- Alloy 820 containing 17.2 percent cobalt, 70.0 percent iron, and 12.8 percent molybdenum. Etched according to procedure 1; transformed alpha in matrix of epsilon phase; epsilon grains smaller than in figure 5. X100.

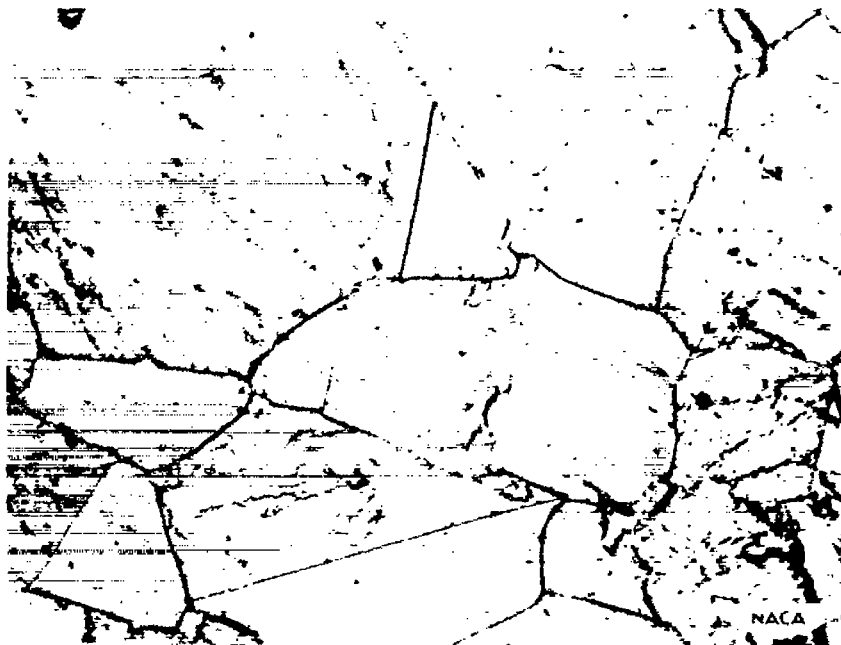


Figure 20.- Alloy 821 containing 18.0 percent cobalt, 70.0 percent iron, and 12.0 percent molybdenum. Etched according to procedure 1; epsilon in matrix of transformed alpha; grain growth is inhibited in alloys consisting of two phases at annealing temperature, resulting in relatively small grain size; X500.

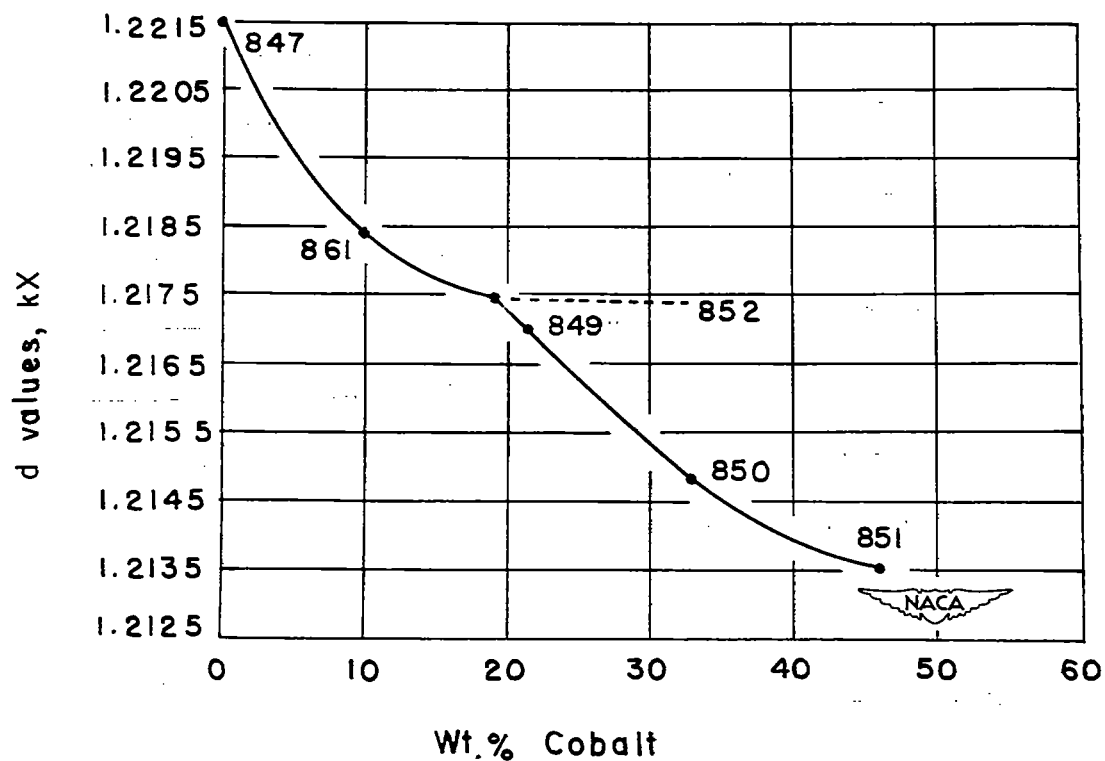


Figure 21.- Variation at 1200° C of the d value of the twenty-ninth X-ray diffraction line of the  $\mu$  phase in the cobalt-iron-molybdenum ternary system plotted as a function of cobalt content.

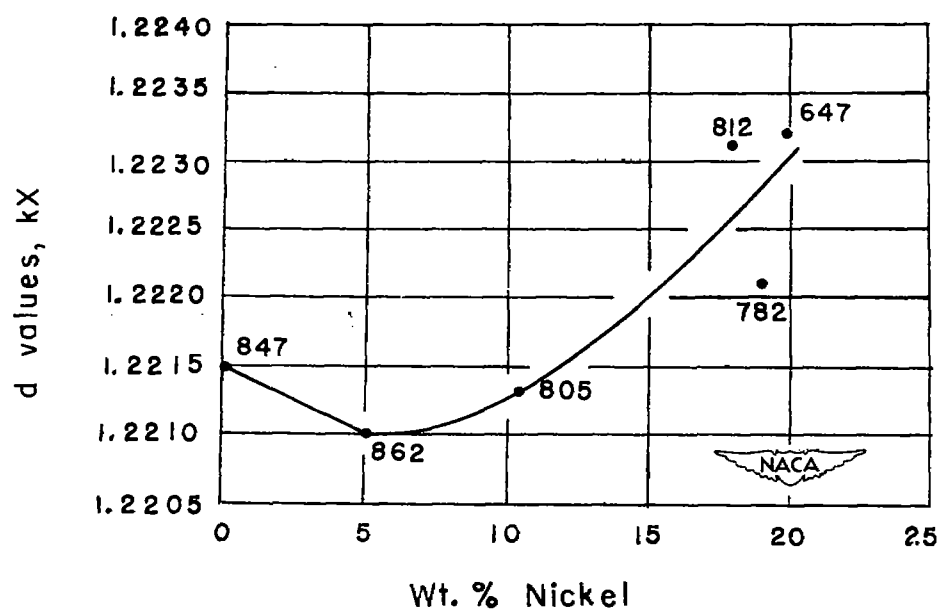


Figure 22.- Variation at 1200° C of the d value of the twenty-ninth X-ray diffraction line of the mu phase in the iron-nickel-molybdenum ternary system plotted as a function of nickel content.

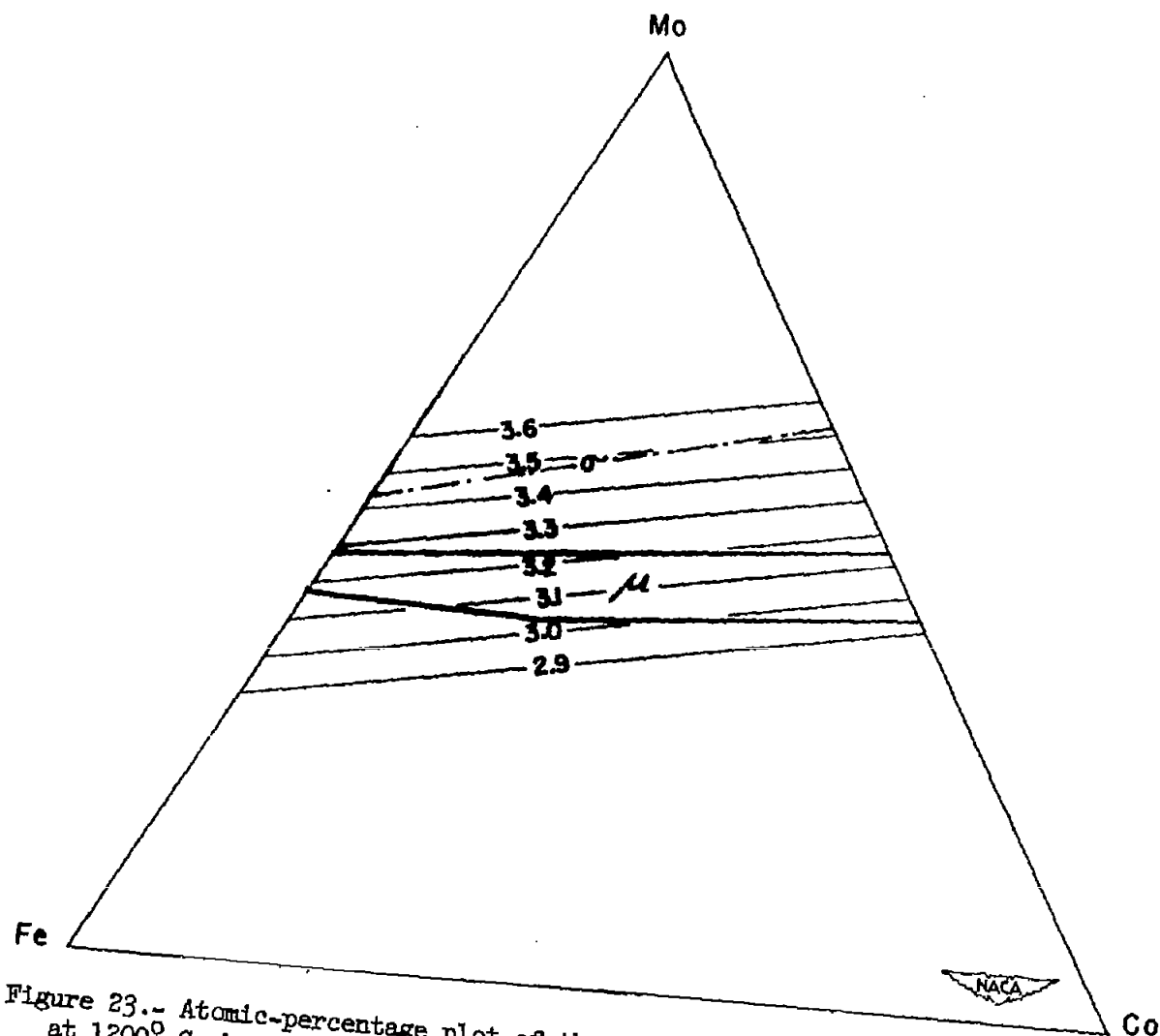


Figure 23.- Atomic-percentage plot of the cobalt-iron-molybdenum ternary system at 1200° C showing location of intermediate phases in relation to electron equivacancy lines.

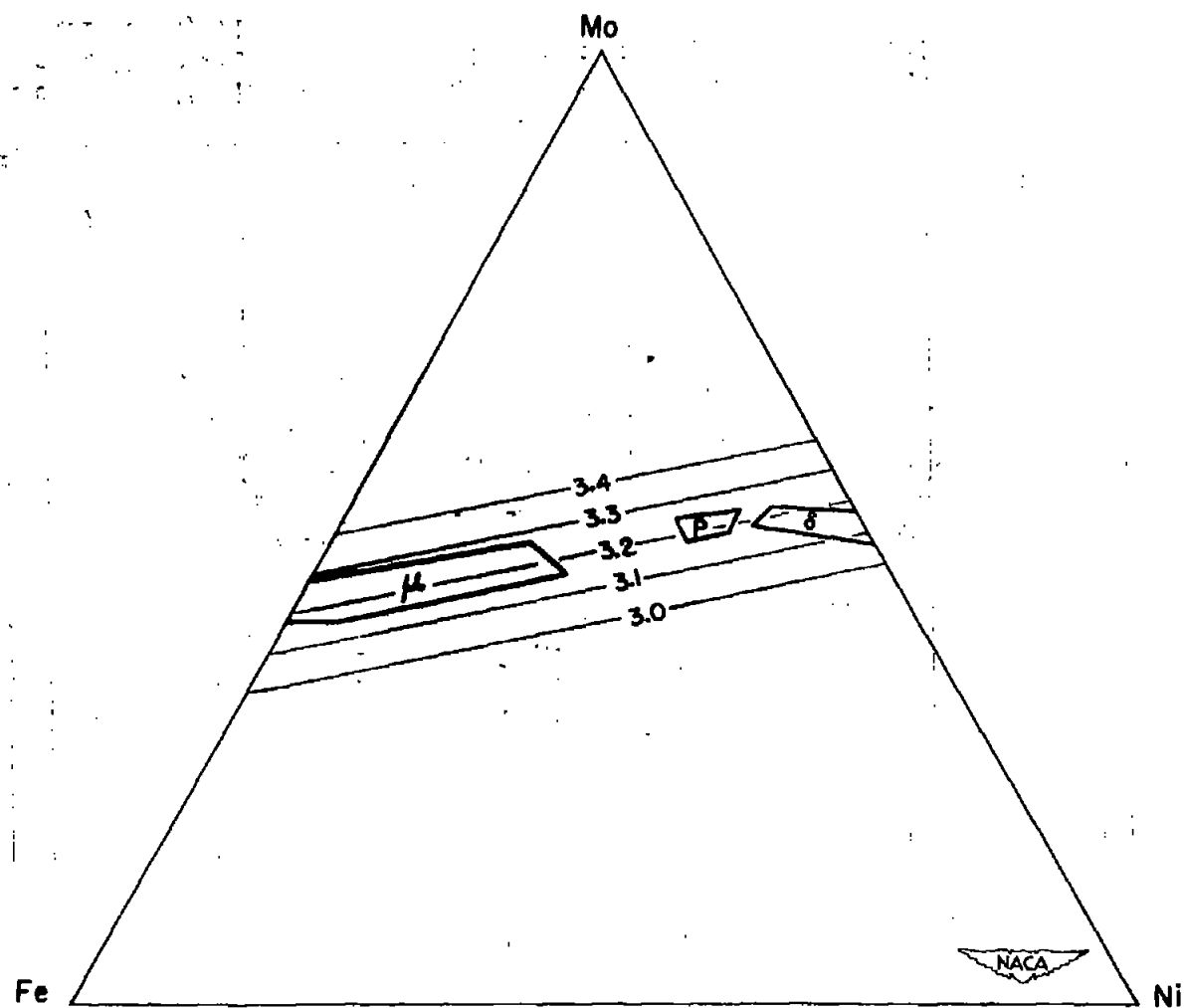


Figure 24.- Atomic-percentage plot of the iron-nickel-molybdenum ternary system at 1200° C showing location of intermediate phases in relation to electron equivacancy lines.

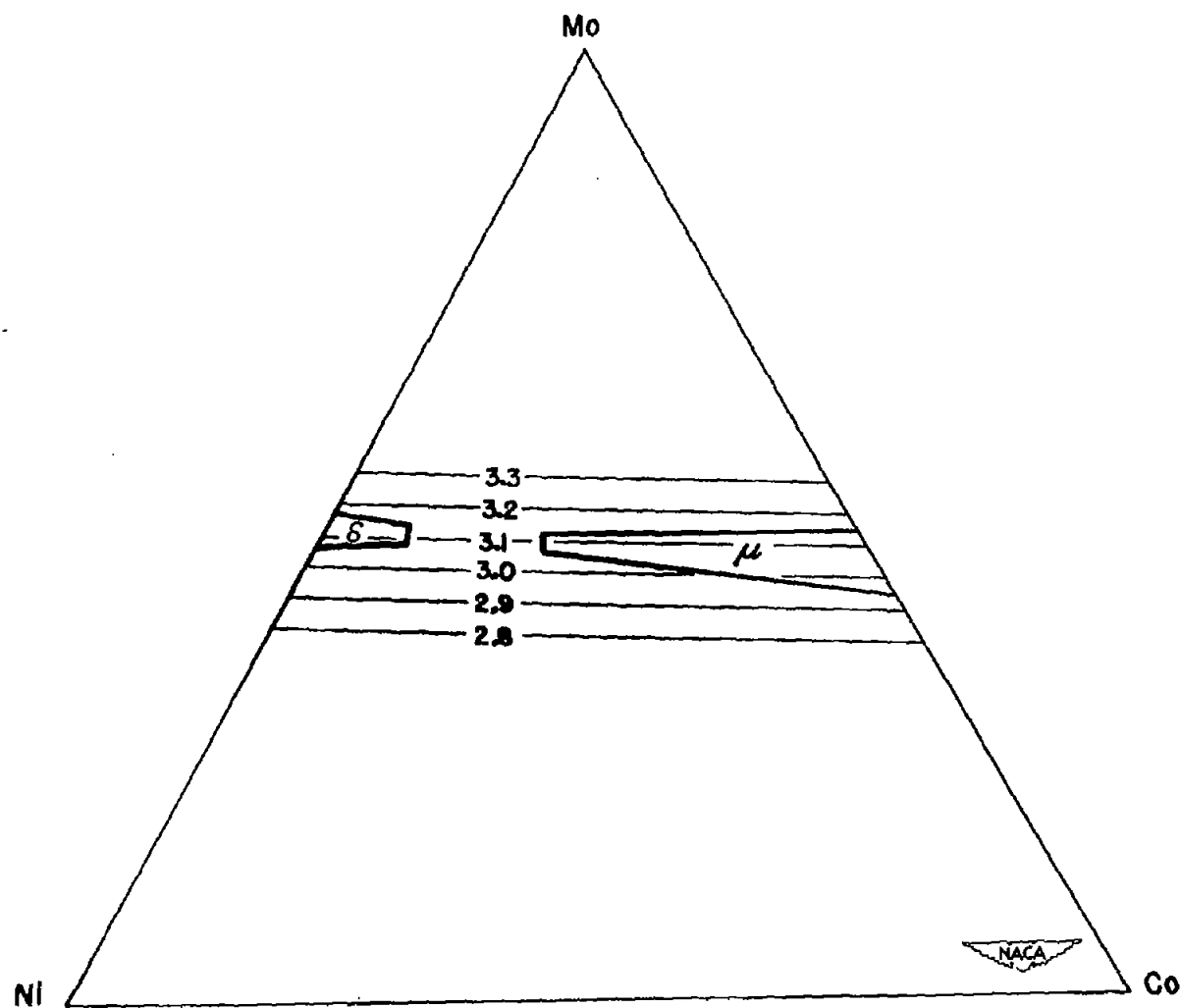


Figure 25.- Atomic-percentage plot of the cobalt-nickel-molybdenum ternary system at 1200° C showing location of intermediate phases in relation to electron equivacancy lines.



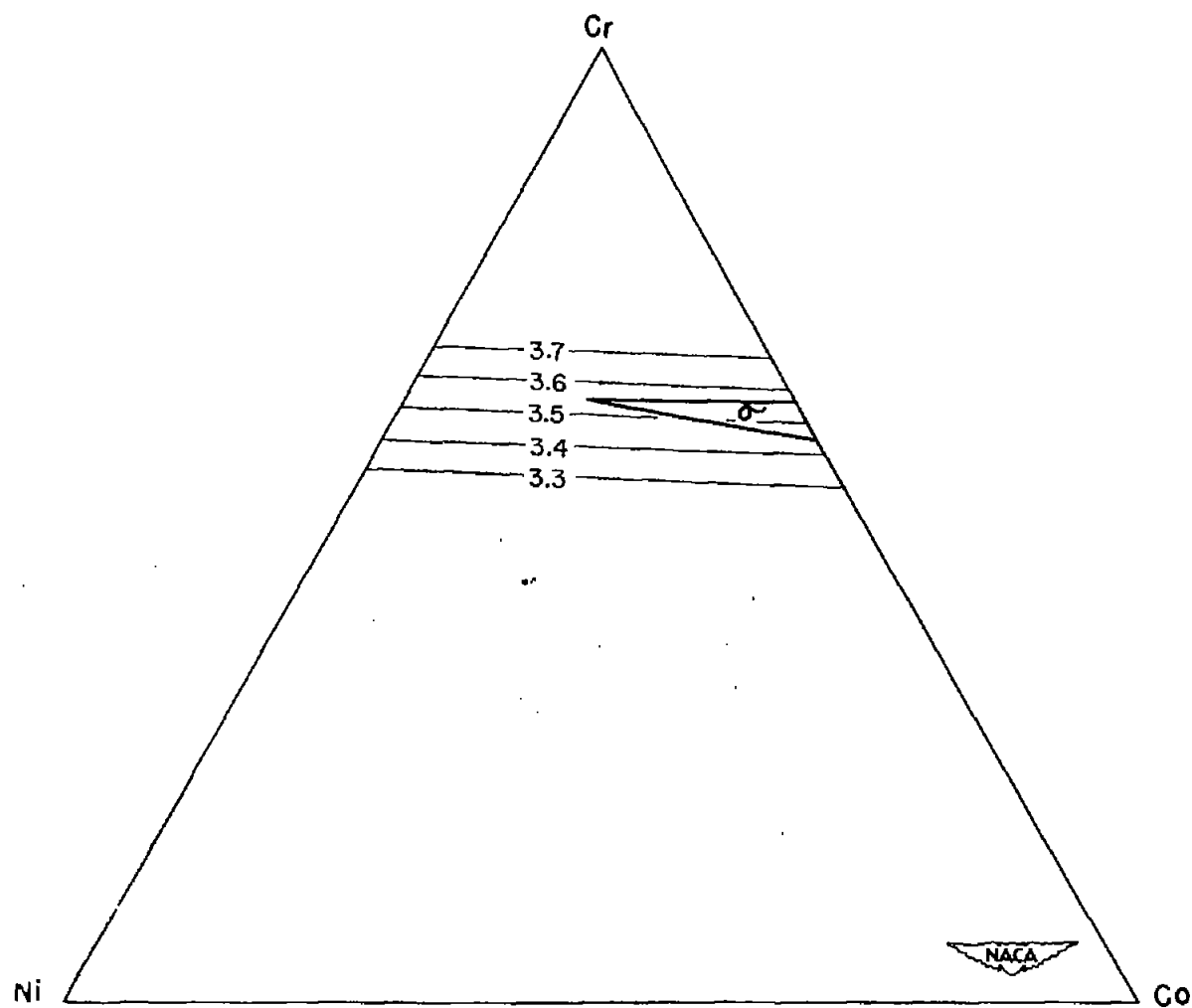


Figure 26.- Atomic-percentage plot of the cobalt-nickel-chromium ternary system at 1200° C showing location of intermediate phases in relation to electron equivacancy lines.